Integrated Master in Chemical Engineering

Modeling and Simulation of Chromatographic Reactors

MSc Thesis

Of

Elson Dinis Gomes

Developed in context of Dissertation curricular unit

Work performed at **BASF SE – GCP/RR**

BASF SE Supervisor: **Dr. Viviana M. T. M. Silva**

FEUP Supervisor: **Dr. Luís Miguel Madeira**

Universidade do Porto
Faculdade de Engenharia
FEUP

Department of Chemical Engineering

July 2014

Acknowledgements

First of all, I wish to thank my supervisor Dr. Viviana M. T. M. Silva for welcoming me at BASF SE, and for all the advice, attention, and guidance she gave me during my internship. All the helpful insights were greatly appreciated and a lot of knowledge was given to me for my future life and career.

I also want to express my appreciation for my Faculty supervisor Dr. Luís Miguel Palma Madeira who made possible this opportunity abroad and believed in me to go on this journey.

Finally, to my close Friends José Monteiro and Patrícia Zhu, for your care and invaluable support in times of need, I thank you. Without you, I would not have made it to where I am now.

Abstract

High added value molecules have always had an important role in our lives and that will continue in the future. The synthesis of these complex molecules is a difficult and laborious process, due to, for instance, limited conversion or low selectivity. These constraints force some industries into exploring natural sources of these molecules to further purify them instead of producing them. High added value molecules are sometimes difficult to synthesize and/or purify. In that sense, chromatographic reactors are powerful contestants in the run for the best units for process intensification since they combine separation with reaction.

Chromatographic reactors are conventionally used to increase conversion in equilibrium-limited reactions. They can also be used in consecutive reactions, in reactions that have inhibiting/poisoning products and also with thermo sensitive compounds like pharmaceuticals. Although there is limited know-how in the subject, some industries already explore the capacities of these reactors in applications such as in bioprocesses, sugar refining, petrochemical (xylenes) and pharmaceuticals (enantiomers).

During this work several chromatographic reactor concepts were simulated. The concepts explored were the Fixed Bed, Reverse Flow and Simulated Moving Bed Chromatographic Reactors. Special attention was given to the Reverse Flow concept and, the Simulated Moving Bed concept was explored to a less extent. All the concepts were tested for a typical esterification reaction known for its limited conversion. The Reverse Flow Chromatographic Reactor (RFCR) seems to overcome the Fixed Bed concept in worse conditions such lower reaction rates and separation factors. RFCR can even be considered over Simulated Moving Bed Reactor (SMBR) systems regarding the simplicity of valve operation and control.

Key words: fixed bed; reverse flow; simulated moving bed; chromatographic reactors; MATLAB®

Resumo

As moléculas de alto valor acrescentado sempre desempenharam um papel importante nas nossas vidas, o que continuará a passar-se no futuro. A síntese destas moléculas complexas é um processo laborioso devido às conversões limitadas e baixas selectividades, por exemplo. Estas limitações fazem com que as indústrias explorem fontes naturais destas moléculas para depois as purificarem em vez de as produzirem de raíz. Portanto estas são difíceis de sintetizar e/ou separar. Neste sentido, os reatores cromatográficos são poderosos candidatos às melhores unidades para intensificação de processos, uma vez que combinam reação com separação.

Os reatores cromatográficos sao usados convencionalmente para o aumento da conversão em reacões limitadas pelo equilíbrio. Podem também ser usados em sistemas com reações consecutivas, em reações com produtos inibidores ou venenosos para o catalisador, e também para compostos sensíveis à temperatura como os princípios ativos de medicamentos. Apesar de haver um know-how limitado, algumas indústrias já exploram as capacidades destes reatores em aplicações como nos bioprocessos, refinação de açucar, petroquímica (xilenos) e farmacêutica (enantiómeros).

Neste trabalho, vários reatores cromatográficos foram simulados. Os conceitos de reator cromatográfico explorados foram o Leito Fixo, Escoamento Reverso e Leito Móvel Simulado. Foi dada expecial atenção ao conceito de Escoamento Reverso aplicada a reações do tipo $A + B \leftrightarrow C + D$ que nunca tinham sido exploradas neste conceito. O reator cromatográfico de leito móvel simulado foi explorado de forma menos detalhada. Todos os conceitos foram testados para uma reação típica de esterificação, conhecida pela sua conversão limitada. Nas simulações efetuadas, o reator de Escoamento Reverso teve desempenhos melhores do que o reator de Leito Fixo em condições de operação menos favoráveis como taxas de reação mais baixas e fatores de separação menores, podendo também apresentar-se como alternative ao reator de Leito móvel simulado devido à sua simplicidade de operação e controlo de válvulas.

Palavras-chave: Leito Fixo; Escoamento Reverso; Leito Móvel Simulado; Reator cromatográfico; MATLAB®

Declaration

I declare under oath that this work is original, and every other source is properly indicated. The majority of the illustrations are original drawings or adaptations from identified sources.

Contents

List of Figures

List of Tables

Notation and Glossary

A	Area of column section	[cm^2]
C_i	Concentration of species i in the liquid	[mol L^{-1}]
D_{ax}	Axial dispersion coefficient	[cm^2 s^{-1}]
k	Kinetic constant	[mol g_{cat}^{-1} s^{-1}]
k'	Kinetic constant ($k' = \rho_b k$)	[mol L^{-1} s^{-1}]
K_{eq}	Equilibrium constant ($A + B \leftrightarrow C + D$)	[-]
$K_{L,i}$	Adsorption constant in Langmuir isotherm	[L mol^{-1}]
L	Column length	[cm]
MW	Molecular Weight	[g mol^{-1}]
Pe	Peclet number (convective/dispersive forces)	[-]
q_i	Concentration of species i in the solid	[mol L^{-1}]
$Q_{L,i}$	Constant for the component i in Langmuir isotherm	[mol L_{ads}^{-1}]
t	Time	[s]
v	Velocity	[cm s^{-1}]
V_{ads}	Volume of adsorbent	[L]
x	Dimensionless length (axial)	[-]
z	Length (axial)	[cm]

Greek Letters

α_{DC}	Separation factor in terms of species D and C	[-]
ε_b	Bulk (or bed) porosity	[-]
ψ	Phase ratio $(1 - \varepsilon_b)/\varepsilon_b$	[-]
ρ_b	Bulk (or bed) density	[g_{cat} L^{-1}]
ρ_i	Density of species i	[g cm^{-3}]
τ	Holdup time L/v_{int}	[s]
θ	Dimensionless time	[-]

Subscripts

ads	adsorbent
ap	apparent
b	relative to bulk or bed
D, des	desorbent (species A)
F	feed
in	in
int	interstitial
b	relative to bulk or bed
R	raffinate
Sup	superficial
X	extract

Superscripts

$*$	denotes equilibrium

Acronyms

BCR	Batch Chromatographic Reactor
CR	Chromatographic Reactor
CSS	Cyclic Steady State
CSTR	Continuous Stirred Tank Reactor
DAE	Differential Algebraic System
DC	Desorbent consumption
FBR	Fixed Bed Reactor
FDM	Finite Differences Method
FORTRAN	programming language (FORmula TRANSlating system)
gPROMS	process development environment (general PROcess Modeling System)
MTBE	Methyl Tert-Butyl Ether
OCFEM	Orthogonal Collocation on Finite Elements Method
PC	Preparative Chromatography
PDE	Partial Differential Equation
pdepe	MATLAB® PDE solver
PR	Productivity
RC	Reactive Chromatography
SMB	Simulated Moving Bed
SMBR	Simulated Moving Bed Reactor
TMB	True Moving Bed
TMBCR	True Moving Bed Reactor
TMC	1,3,5-Trimethylcyclohexane
VOC	Volatile Organic Compounds
RFCR	Reverse Flow Chromatographic Reactor

1. Introduction

1.1. Relevance and Motivation

The present work deals with modeling and simulation of Chromatographic Reactors in MATLAB®. Three major concepts are analyzed: Fixed Bed Chromatographic Reactor (FBCR), Reverse Flow Chromatographic Reactor (RFCR) and Simulated Moving Bed Reactor (SMBR). Equilibrium-limited reactions are very common and can significantly be improved using hybrid processes. Membrane reactors, Reactive Chromatography and Reactive Distillation are possible alternatives with the latter being the process of choice in a high number of industrial applications. Nevertheless chromatographic and membrane reactors are gaining relevance, particularly for bio-processes, thermo labile substances and reactions with inhibiting/poisoning product. Usually, in bioprocesses, where high molecular weight products are desired, traditional methods of separation like distillation are not suitable. By combining reaction with chromatographic separation, equilibrium-limited reactions can be enhanced, in some cases until complete conversion of reactants. This way the reverse reaction is prevented due to the displacement of the products from the reaction zone. Some significant advantages of chromatographic reactors are that high purity products can be isolated and, separations can be made at relatively low temperatures and pressures, which are very important details when sensible compounds are involved, particularly high added value products. Some of the advantages and disadvantages of Reactive Chromatography are summarized in Table 1-1**Error! Reference source not found.**.

In industrial environments, modeling and simulation is used as a mean of reducing the costs and saving time spent on process development, allowing for a first approximation of the results that could be expected from such processes. Also, modeling and simulation can be used to develop control strategies and perform optimization on existing processes (Litto et al., 2006). Dynamic modeling is important for reactor start up and shut down, for studies on stability (upon disturbances) and mostly because some processes operate in dynamic mode like the chromatographic reactors presented in this work. Knowledge of reactor behavior is essential for making changes that ideally will lead to increased performance.

Table 1-1 – Advantages and disadvantages of chromatographic reactors.

Advantages	Disadvantages
Integration reduces equipment costs	Complex dynamics and control systems (not always)
In-situ adsorption drives reactions beyond equilibrium	Narrow range of operation of adsorbents (T and P)
Conversion of difficult separable components	Loss of degrees of freedom and flexibility
Avoids the destruction of sensible molecules (low T and P)	Product separation and recovery is needed
Extendable to multi-component separations	Sometimes high grade eluent is needed
Lower desorbent consumption in SMBR	Dilution and discontinuity in batch operation

1.2. Work Contributions

BASF has been a leading company on attending to customers' requests. The growing demand for functionalized materials and customized solutions is making BASF shift its drive from classical chemicals towards this new direction. This is an area of high added value products as opposed to bulk chemicals. High added value chemicals tend to have specific characteristics (complex total synthesis, difficult separation, degradability) that make them challenging to produce. In that perspective chromatographic reactors are key candidates to help overcome these production constraints. Reverse flow chromatographic reactors (RFCR) are a commonly less discussed alternative in reactive chromatography systems, but they may pose improvements compared to fixed bed chromatographic reactors (FBCR) and even to simulated moving bed reactor (SMBR) systems which are more complex to operate. Therefore the thesis presented attempts to make clarifying contributions to this topic using MATLAB® based tools.

Several tools were considered at the beginning of this work. The first approach to simulation was made with MATLAB® PDE Toolbox but this was not as flexible as intended. Also, the inability to solve advection-diffusion-reaction-adsorption equations combined with the inability of solving large systems of partial differential equations led to the exclusion of PDE Toolbox from the range of options considered. The PDE intrinsic solver of MATLAB®, *pdepe*, proved to be quite flexible for implementation of the different concepts. Although *pdepe* also revealed limitations, it is a fast and efficient way of predicting dynamic behavior.

1.3. Thesis Organization

The relevance and major contributions of this work are presented in *Chapter 1*. A description of operation modes of different types of chromatographic reactors simulated and respective applications are presented in *Chapter 2*; it is basically a short state of the art about operation and applications of chromatographic reactors. The concepts explored are the FBCR, RFCR and SMBR. A brief description of the Batch CR is also provided as introduction. The modeling and the simulation of chromatographic reactors is addressed in *Chapter 3*. The pseudo-homogeneous model is presented. Also, the explored numerical tool flexibility is explained in detail so that it can be extended to other possible concepts to implement. Since conservation of mass is important in chemical systems, the error associated with the tool used is tested by tracer experiment simulation. *Chapter 4* presents the simulation results for the concepts explored, FBCR and RFCR (and to a less extent SMBR), and attempts to extract information on reactor performance through comparison between those two. Some insight on how the reactors may behave under specific operating conditions is also given. Finally, in *Chapter 5*

concluding remarks are made regarding all the work developed and suggestions for future improvements are also given.

2. State of the Art of Chromatographic Reactors

A review on operation and applications of different types of chromatographic reactors is presented. The focus is given to Fixed Bed Chromatographic Reactor (FBCR), Reverse Flow Chromatographic Reactor (RFCR) and Simulated Moving Bed Reactor (SMBR).

2.1. Principles and Operation

Chromatographic reactors integrate the reaction and separation steps in the same unit. Since the products leave the column at different times they can be collected to separate tanks, reducing the scale of purification/concentration efforts. But this is only true for FBCR and RFCR systems, not for SMBR where constant streams of raffinate and extract are collected at the same time. The same applies for the annular chromatographic reactor.

The differences in affinity towards the adsorbent will cause the different molecules to travel with different velocities along the column thus being separated after some distance/time. Ideally, at least one of the products should be easily carried away from the reaction zone so that the reaction never reaches equilibrium, proceeding until complete conversion (Levan and Carta, 2008; Podgornik and Tennikova, 2002). Consecutive reactions are also enhanced since a specific intermediate species can be drawn off avoiding low yield/selectivity.

The best way of understanding what goes on inside the chromatographic reactor is explained when a reaction of the type $A \leftrightarrow B + C$ takes place, as illustrated for the case of a batch chromatographic reactor (BCR) in Figure 2-1. Here, the batch designation is related with the fact that the operation mode is discontinuous or pulsated. With a simple experiment in which a pulse of reactant A is fed to the column, we can see its behavior through the elution profiles. Reactant A divides itself into two different molecules B and C and, since the packing has both catalytic and adsorptive properties, all species will suffer a different delay.

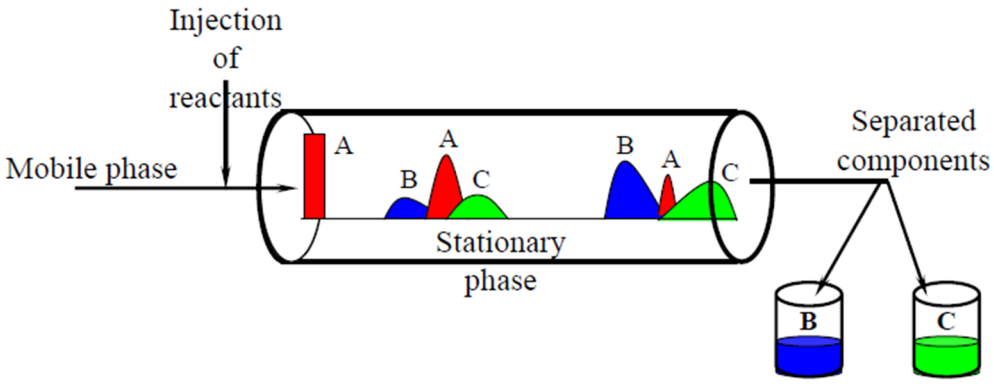

Figure 2-1 – BCR operation $A \leftrightarrow B + C$ (Seidel-Morgenstern, 2013).

Supposing that A is more retained than B and less than C, the elution profiles, or if preferred, the times of elution of each species, will be on the following order $t_C^{elution} < t_A^{elution} < t_B^{elution}$. This can also be seen in Figure 2-1. When B and C are formed, the latter will be traveling in the front of A while the former behind. With this we can see that given a sufficient length of column (Silveston and Hudgins, 2012), A will be completely reacted, and additionally B is completely separated from C.

The separation of the consecutive pulses in two different peaks enables the collection of the two different species at the outlet. Like previously said, if the pulses are given enough time, the peaks will separate completely. The successive pulses should be injected after some time interval enough so that the faster travelling compound will not overlap the slowest one near the column outlet. If the column is too short and/or the pulses are fed more frequently than what they should, the peaks will overlay as seen in Figure 2-2. The zones of the chromatogram that overlay mark the fraction of outflow that should be recycled because it contains unreacted A and products B and C. So, ideally, the collection of different fractions at the outlet would be alternate, as illustrated below.

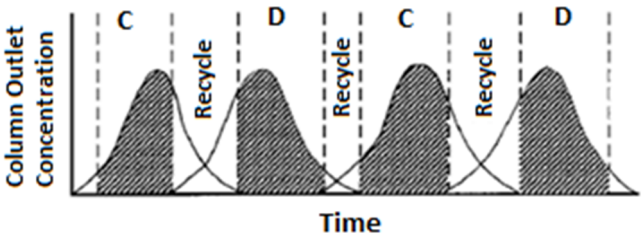

Figure 2-2 – Chromatogram and fractionation scheme for the BCR operating in pulse mode. Reaction of the type $\boldsymbol{A \leftrightarrow B + C}$ adapted from (Levan and Carta, 2008).

Other cases can be interesting as well if A has not an intermediate affinity towards the adsorbent. In these situations, the operation of the column might be somehow different. Usually the adsorbent is selected with these limitations in mind, in order to optimize the reaction and separation, which could be translated in decreased column length and desorbent consumption, or more importantly, improved product purity. Typical examples for the catalysts are enzymes and metals supported on other materials, usually an adsorbent. There are also other materials that act both as adsorbent and catalyst like zeolites and ion-exchange resins. Other adsorbents that might be used include activated carbon and alumina. The packing delivering higher conversion ratios is the homogeneous mixture of catalyst and adsorbent or a material that serves as both like resins (Podgornik and Tennikova, 2002).

The major drawbacks of the batch operation mode, presented above, are eluent consumption and non-continuous product streams. In order to increase BCR production, several pulses are injected in order to get an outlet composition like that of Figure 2-2. Also, the injected pulse should be as large as possible to save desorbent. These measures are useful but other arrangements were developed to

improve chromatographic reactor performance. Alternative arrangements are the RFCR and SMBR which will be explained later.

Usually chromatographic reactors are operated in a cyclic manner, due to the necessity of regeneration steps. In the case of FBCR and RFCR It is noteworthy that column regeneration can spend a significant portion of the complete cycle (feed + regeneration). The favourable isotherm character for the adsorption will have an unfavourable character while desorption is taking place. This is why the regeneration step lasts longer than the feed step. For the SMBR system the regeneration is achieved in a continuous way at the same time as products are retrieved. Design methods for cycles rely on mathematical modeling and often extensive lab/pilot plant experiments (Levan and Carta, 2008).

In a real experiment or industrial installation, a reliable on-line detection method needs to be put in place so that a fractionating valve could separate the eluant into different fractions (FBCR and RFCR). Generally time based fractionation is used but if possible the cuts should be made according to concentration measurements.

2.2. Types of Chromatographic Reactors

2.2.1. Fixed Bed Chromatographic Reactor(FBCR)

The FBCR is the same fixed bed has in the previous arrangement and is also operated in an easy way; normally two or more columns are used in parallel to allow regeneration to occur at the same time of production. The main difference compared with the batch chromatographic reactor is the operation mode, such that it operates with a longer feed step. The feed is provided until a specific product or reactant starts to elute. There are two distinct phases of operation, feed and regeneration as illustrated in Figure 2-3 for the reaction type $A + B \leftrightarrow C + D$. During the first phase, the column is fed with the reactive mixture until some point in time when the concentration profiles no longer change and regeneration starts (second phase). In order to optimize performance, other switching conditions can also be defined, like reactant or undesired product eluting instead. The production and regeneration times are directly connected to the type of reaction taking place, meaning that they are specific to each compound, adsorbent and affinities and, consequently, these times are going to be different. Ideally, column regeneration phase should take the same as the production phase in order to reduce nonproductive periods. This can be accomplished with the increase of flow rate in the regeneration period.

During the production and regeneration stages, several fractions can be collected at the outlet, in order to attain the desired separation. This separation is possible due to the differences in the affinities of species for the adsorbent material. A fractionation scheme is also given in Figure 2-3 so that

this process can be better understood. The red vertical lines mark the time periods at which the fractionation valve switches between the tanks that collect the different fractions. The fractions from the beginning of the feed until the first valve switch is the desorbent recycle, from the first to the second switch (left image) the raffinate is collected, after this, the inlet is switched to pure eluent, and until the next valve switch (right image) the mixture to be recycled is collected; the last fraction is collected until the column is completely regenerated. After this a new feed step can be initiated.

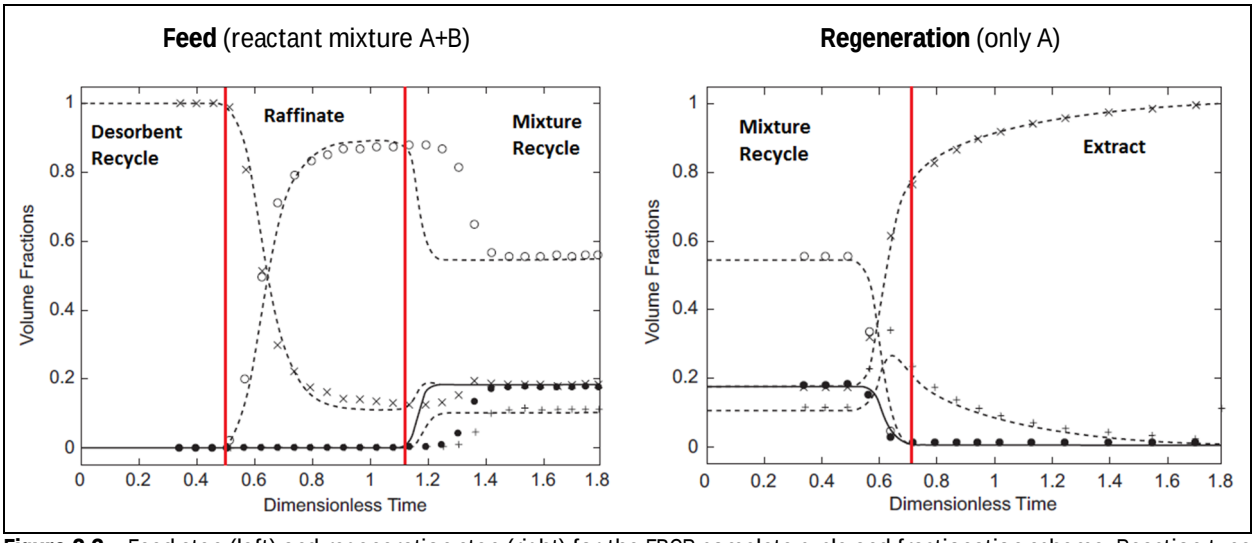

Figure 2-3 – Feed step (left) and regeneration step (right) for the FBCR complete cycle and fractionation scheme. Reaction type $\boldsymbol{A} + \boldsymbol{B} \leftrightarrow \boldsymbol{C} + \boldsymbol{D}$. (x) – A, (•) – B, (o) – C and (+) – D. (adapted from (Mazzotti et al., 1997)).

It is now clear that the FBCR should be operated in a cyclic way, preferably with paired similar units for the continuous production; while one is on the feeding phase, other(s) is(are) in the regenerating phase.

The purity of Raffinate and Extract fractions is determined by the times at when the cuts are made which is explored later on this study. For higher purity of fractions, careful attention to concentration tolerances is paid, causing a lot of main product to be recycled and inherently a decrease in productivity. For increased productivity, fraction collection times are somehow longer, decreasing purity of raffinate and extract stream fractions. A compromise between the two has to be met. Generally, high purity is desired rather than high throughput, avoiding further costs in the operation of downstream separating units.

2.2.2. Reverse Flow Chromatographic Reactor (RFCR)

The configuration of a RFCR is basically a column with the feed located exactly at half the total length, or a pair of two columns interconnected and the feed in this interconnection. The operation mode of the RFCR is better understood with Figure 2-4 and Figure 2-5. At the first half cycle (left image), the carrier coming from the left side of the column pushes the reactants towards the outlet on the

opposite side. The outlet coming from the left or right sides is directed to a fractionation valve that collects the different fractions. If the adsorbent has a high affinity towards the reactant it is trapped in the middle section of the RFCR.

This type of reactor is extensively used with environmental concerns for gas phase reactions as is the case of VOC's oxidation. VOC's are trapped inside until complete oxidation. The same is explored for ammonia in liquid phase. These are irreversible reactions of the type $A + B \rightarrow C$. In the case of VOC's or ammonia, the packing catalyzes their oxidation and at the same time delays their appearance at the outlet, and when they reach the outlet the flow is reversed. The interest in this case is also related to the trapping effect of the heat inside the reactor keeping the bed at a desired temperature.

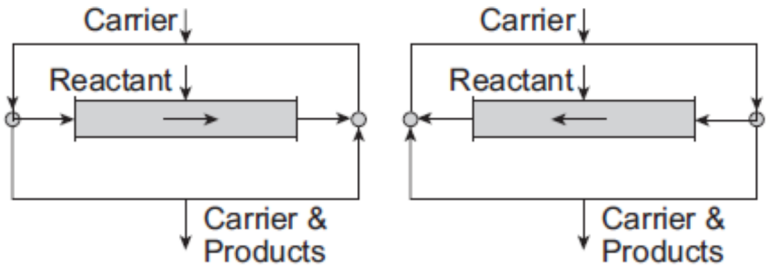

Figure 2-4 – RFCR operation mode. Adapted from (Viecco and Caram, 2006).

The concept was never explored for a reaction of the type $A + B \leftrightarrow C + D$. The same principles explained above are applied, but in this case a full regeneration step has to be performed to rid the column from the most retained species, but less frequently than the FBCR.

In Figure 2-5, it is more intuitive how the RFCR is operated and should be modeled. The illustration is only valid before the reversal. There is a desorbent/eluent inlet at one extremity, say left, a feed inlet in the middle, and also an outlet at the opposite side of the inlet of desorbent. The feed mixture is fed to the reactor's second column/second half and when the front of some specific compound is reaching the outlet, the flow of desorbent is reversed and the eluate fronts start to move on the opposite direction or inside the other column/section. This is simply done by switching both inlet and outlet valves at the same time. The feed is continuous and a mass balance is made for each species where the feed meets the outlet of a column and this mixture is fed to the following column. Both columns have different operating conditions although the packing is the same. The collection vases are also represented as a first attempt of explaining the outlet fractionation scheme presented latter.

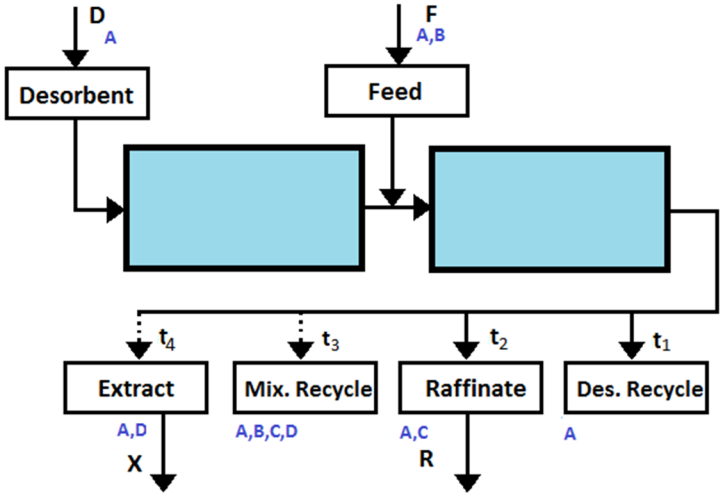

Figure 2-5 – RFCR scheme for reaction $\boldsymbol{A} + \boldsymbol{B} \leftrightarrow \boldsymbol{C} + \boldsymbol{D}$ with collection tanks.

The control and operation of this type of reactor are simpler than that of an SMBR due to the fact that there are not so many valves to operate, thus reducing chances of failure, becoming more robust than the latter.

2.2.3. Simulated Moving Bed Reactor (SMBR)

The disadvantages of batch systems lead to the development of continuous production systems like the True Moving Bed (TMB), which evolved into the Simulated Moving Bed (SMB) mainly because of difficulties originated with the moving of solids. The SMBR is composed of at least four FBCR interconnected in a loop arrangement, allowing continuous production. Several columns per section are also applied or even different number of columns in each section depending on the relative separation factors of mixture components. As the name says, the SMBR operates in a way that movement of solids is simulated.

Simulation of the solids is done by switching every outlet and inlet frontward by one position through a scheme of valve switching. At the eyes of someone located at section II, after the first switch, the feed is further away from that column on which the more strongly adsorbed species is retained. The first cycle is completed when for instance the feed returns to the same position as in the beginning of the cycle, so for the simplest SMBR, the cycle is completed after four port switches. The control of such valve system is complex and prone to failure, and also these valves are even more expensive if they are suited to operate at moderate temperature and pressure, which limits the applicability of such intensive process.

The SMBR configuration and its simplest mode of operation are comprehended best by inspection of Figure 2-6.There are two main regions the first I&IV, is called regeneration/recycling zone

and the other II&III is a separation /reaction zone. The feed containing the reactants and/or other compounds has its inlet located between section II and III. The less retained compound is collected between sections III and IV, and the most adsorbed compound is collected between section I and II. The desorbent is added to the stream that leaves column IV, which should be free of any eluate.

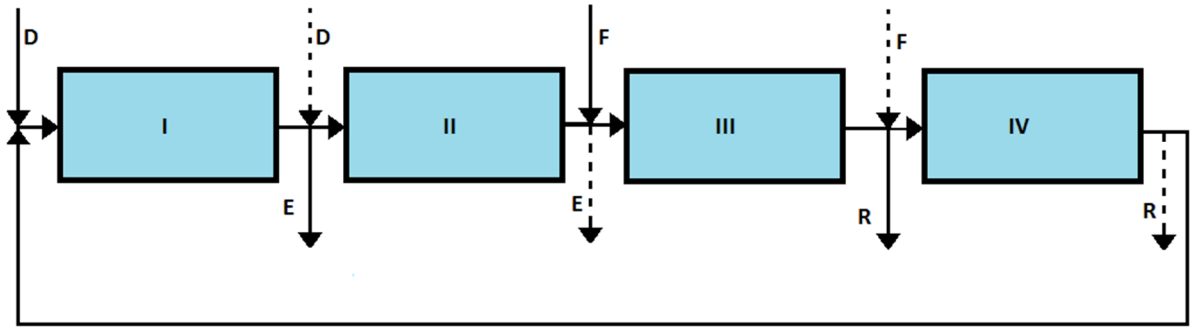

Figure 2-6 – Scheme of an SMBR. Solid line – first stage, dashed line – second stage. F-feed, D-desorbent, E-Extract, R-raffinate.

Because of its ability of combining difficult separations and reactions limited by equilibrium, SMBR became one of the most studied types of Chromatographic reactor by far. Also, it was shown that for irreversible reactions the use of SMBR increased conversion, avoiding temperature and pressure rises (Ganetsos et al., 1993). Reactive variable section length systems could produce a higher purity product for a fixed yield, and consume slightly less eluent in the high purity region than more rigid SMB systems (Yu et al., 2003).

SMBR types of reactors are typically operated in a cyclic way, in the sense that after a number of ports switched the feed is at the same position as in the beginning; this constitutes a complete cycle. The concentration profiles in the different sections, after a determined number of cycles, start and end up with the same profile shape after each port switch. When this is observed it is said that the Cyclic Steady State (CSS) was reached.

2.3. Applications

Since the first chromatographic reactors were introduced and patented by Dinwiddie James and Morgan Walter, several improvements were made to this technology which will be discussed in this work. Several patents were filed at relatively the same time in two different continents as can be seen in Table 2-1Table 2-1 – First Chromatographic Reactor Patents. The patent presented first, by Dinwiddie, is a type of reactor resembling that of the annular chromatographic reactor. It was designed for dehydrogenation of butene mixtures on which there is a rotating arm that distributes the reactants over the packing, cf. Figure 2-7. Dinwiddie claimed that hydrogen resulting from the reaction was separated continuously shifting the equilibrium of the reaction towards the formation of butadiene. The

second patent by Magee consisted of a fixed bed for reaction in gas phase operating in a pulsated way. The examples given were the reverse water-gas shift reaction and the conversion of hydrogen chloride to chlorine. Magee even gave a description of the fractions being separated along the column, cf. Figure 2-8.

Table 2-1 – First Chromatographic Reactor Patents

Authors	Year	Patent Number
J.A. Dinwiddie, W.A. Morgan	1961	U.S. Patent 2 976 132
E.M. Magee	1961	Canadian Patent 631 882
G.A. Gaziev, S.Z. Roginskii, M.J. Yanovskii	1962	U.S.S.R. Patent 149 398

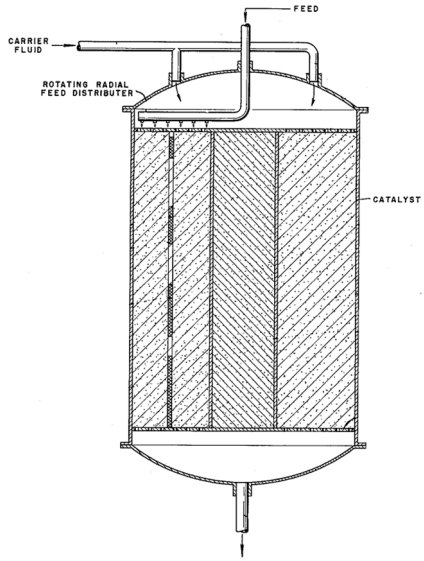

Figure 2-7 – Annular chromatographic reactor by (Dinwiddie, 1961).

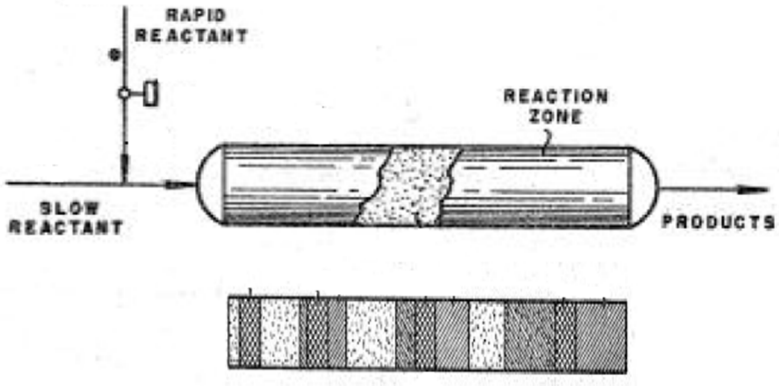

Figure 2-8 – Fixed bed column operating with pulsated feed (Magee, 1961).

Chromatographic reactors are used essentially when the reaction is limited by equilibrium, in the case of consecutive reactions, reactions involving temperature-sensitive compounds and reactions with inhibiting/poisoning product. Although Chromatographic reactors have drawn a lot of attention, their application in industry has not been significant due to lack of enough studies concerning its difficult design (Falk and Seidel-Morgenstern, 2002; Javeed et al., 2011; Vu and Seidel-Morgenstern, 2011).

The great majority of applications studies are focused on the FBCR. Lately, the attention has been shifted to the SMBR technology. Reverse flow applications are less common in literature, despite that, Table 2-2 summarizes some of those. Chromatographic Reactors are used in several industrial processes, more or less well established. Examples are the isomerization of C_8 oil products and subsequent separation. In this particular case of C_8 separation it is very attractive compared to reactive distillation since these compounds tend to have very similar boiling points and thus the columns for this kind of separation would have a lot of stages. It is worth noticing that all major applications of SMBR

evolved naturally from SMB separation processes. A lot of knowledge has already been collected since the first chromatographic reactors so, in the future, a larger number of applications is expected to be available including industrial ones. Table 2-2 shows some of the recent applications of SMBR technology.

Bio-refineries will have a decisive role in the future. Lignin breakage products lead to complex mixtures. These mixtures could be enhanced using a chromatographic reactor which could convert low value molecules into high grade and useful ones. Groups of compounds having close retention times could also be collected in the same fraction and further converted in similar units.

Table 2-2 – Chromatographic reactors' applications.

Reaction Type	Product	Adsorbent and / or Catalyst	Reactor Type	Reference
Esterification / Hydrolysis	Menthyle Acetate	Resin	Fixed Bed	(Sardin and Villermaux, 1985)
	Ethyl acetate	Amberlyst 15	Fixed Bed	(Mazzotti et al., 1997)
	Acetic acid methanol	Amberlyst 15	Fixed Bed	(Sircar and Rao, 1999)
	Formic acid methanol	DOWEX 50W-X8	Fixed Bed	(Falk and Seidel-Morgenstern, 1999)
	Formic and acetic acid methanol and ethanol	DOWEX 50W-X8	Fixed Bed	(Mai et al., 2004)
	Beta-Phenethyl acetate	na	SMB	(Kawase et al., 1996)
	Methanol & Formic Acid	DOWEX 50W-X8	SMB	(Vu and Seidel-Morgenstern, 2011) (Falk and Seidel-Morgenstern, 2002)
Etherification	MTBE	Amberlyst 15	SMB	(Zhang et al., 2001)
Acetalization	Diethyl acetal	Amberlyst 18/15	SMB	(Silva and Rodrigues, 2005)
Oxidation	Amonia	Al_2O_3/V_2O_5	Reverse Flow	(Agar and Ruppel, 1988)
Inversion / Isomerization	Isopentane	Zeolite	Reverse Flow	(Viecco and Caram, 2006)
	Monosaccharide	Resin (FINEX)	SMB	(Borges da Silva et al., 2006)
	Lacto-sucrose	Enzyme	SMB	(Kawase, 2001)
	Dextran	na	SMB	(Barker et al., 1992)
	Monosaccharide	na	SMB	(Azevedo and Rodrigues, 2001)
	Monosaccharide	Resin/Invertase	SMB	(Kurup et al., 2005)
	p-xylene	Zeolite	SMB	(Minceva et al., 2008)
Condensation	Ethane & Ethylene	Sm_2O_3	SMB	(Tonkovich and Carr, 1994)
	Bisphenol-A	Resin	SMB	(Kawase et al., 1999)
Hydrogenation	TMC	Chromosorb 106/Pt-Al_2O_3	SMB	(Ray and Carr, 1995)

3. Modeling and Simulation

3.1. Modeling

Modeling and simulation works as a prelude to pilot plant behavior or scale-up operations. Through these, industry is able to diminish costs, to save time spent on development, and to reduce as well the number of experiments which are always required. Another advantage is that it can be used to perform parametric tests. Also, modeling and simulation can be used to develop control strategies and perform optimization on existing processes (Litto et al., 2006). Dynamic modeling is important for reactor start up and shut down, studies on stability (disturbances) and mostly because some processes operate in dynamic mode like chromatographic reactors presented in this work.

The equilibrium dispersive model employed herein does not account directly for the effect of a different phase or considers the mass transfer limitations; they are all lumped in a single apparent dispersion factor. It is assumed that all mass transfer limitations can be represented by D_{ax}. Several other assumptions are made to describe the model used. The assumptions made in this model were:

- Lumped Broadening Effects (D_{ax}).
- Isothermal operation.
- Homogeneous packed column.
- No gradients in radial direction.
- Constant volumetric flow rate.
- Instantaneous equilibrium of adsorption.

For the model assumptions made above, the resulting differential equation (3.1), adapted from (Javeed et al., 2012), is obtained:

$$\frac{\partial C_i}{\partial t} = D_{ax}\frac{\partial^2 C_i}{\partial z^2} - u_i\frac{\partial C_i}{\partial z} - \psi\frac{\partial q_i^*}{\partial t} + \psi\nu_i R \tag{3.1}$$

with

$$\psi = \left(\frac{1-\varepsilon}{\varepsilon}\right) \tag{3.2}$$

and

$$R = k'\left(C_A C_B - \frac{C_C C_D}{K_{eq}}\right) \tag{3.3}$$

where C_i is the concentration of every intervening species, D_{ax} is the axial dispersion coefficient, u_i is the interstitial velocity, q_i^* is the concentration in the solid in equilibrium with the liquid concentration, ψ is a phase ratio, ε is the porosity of the bed, k' is the kinetic constant k multiplied by the bed density

ρ_b, K_{eq} is the reaction equilibrium constant and ν_i is the stoichiometric coefficient having negative sign for reagents and positive sign for products.

In dimensionless form (except concentration), with $\theta = t/\tau$; $x = z/L$; $\tau = \varepsilon L/u_o = L/u_i$, the following equation results:

$$\left(1 + \psi\frac{\partial q_i^*}{\partial C_i}\right)\frac{\partial C_i}{\partial \theta} = \frac{1}{\text{Pe}}\frac{\partial^2 C_i}{\partial x^2} - \frac{\partial C_i}{\partial x} + \psi\nu_i\tau R \tag{3.4}$$

where τ is the holdup time, L is the column length, θ and x are the dimensionless time and length variables, respectively.

The model to implement is determined by the level of accuracy with which we want to describe the physical phenomena. The more describing the model is, the more difficult it is to solve it numerically. The presence of diffusive terms in the system of equations has a beneficial effect on the numerical treatment. Diffusion smoothens the solution and reduces difficulties associated with the approximation of the convection terms, since this term is problematic for some numerical methods. A resume of difficulties arising during the development of models is presented in the list below:

- Large number of equations
- Strongly coupled equations
- Very sparse matrices
- Reaction stiffness
- Numerical diffusion (introduced by convection approximations)
- Oscillation (steep gradients and discontinuities, moving fronts)
- Good looking but fake solutions

The model explored in this work is an equilibrium dispersive one and it was used to simulate all the chromatographic reactor types considered. The choice of this model was based on its simplicity and known ability to describe chromatographic reactor models (Javeed et al., 2011). Alternatively, some authors represent equal systems by a model of N tanks in series which can be described by an ODE in time for each component in each tank (Viecco and Caram, 2006).

The adsorption isotherm used throughout this work is a multicomponent Langmuir isotherm given by equation (3.5),

$$q_i^* = \frac{Q_{L,i}K_{L,i}C_i}{1 + \sum_j^n K_{L,j}C_j} \tag{3.5}$$

where q_i^* is the species concentration in the solid phase in equilibrium with the liquid concentration, $Q_{L,i}$ is the maximum adsorption attainable for the species i, $K_{L,i}$ is the affinity constant for the species i and n is the number of species present that interact with the desorbent.

The simulations were performed for the reaction type $A + B \leftrightarrow C + D$ in which A is also the desorbent. Data for Langmuir isotherms in Table 3-1 was collected from a paper dealing with ethyl lactate synthesis (Pereira et al., 2009).

Table 3-1 – Multicomponent Langmuir isotherm parameters (Pereira et al., 2009).

Component	$Q_{L,i}$ $[mol\ L^{-1}]$	$K_{L,i}$ $[L\ mol^{-1}]$
A (ethanol)	6.299	3.068
B (lactic acid)	4.943	4.085
C (ethyl lactate)	3.237	1.815
D (water)	20.584	7.055

The column parameters used in all simulations were $L = 25\ cm$, $A = 5.31\ cm^2$ with $\varepsilon_b = 0.4$.

3.1.1. FBCR

3.1.1.1. Initial and Boundary conditions

The initial condition is that the bed is saturated with A, the same as saying that $C_A = 17.126M\ \forall x$. At the inlet, the conditions change on the same run and are given in Table (3.2). These conditions are also based in the same paper from which the isotherm parameters were taken.

Table 3-2 – Inlet conditions for the first run of the FBCR.

$\theta \leq \Delta\theta_{feed}$	$\theta \geq \Delta\theta_{feed}$
$C_{A,0} = 7.514M$ $C_{B,0} = 7.514M$ $C_{C,0} = C_{D,0} = 0$	$C_{A,0} = 17.126M$ $C_{B,0} = C_{C,0} = C_{D,0} = 0$

The Danckwerts boundary conditions (3.6) and (3.7) apply for every species *i*:

$$C_{i,0} = C_i - \frac{1}{Pe}\frac{\partial C_i}{\partial x}\bigg|_{x=0} \tag{3.6}$$

and

$$\frac{\partial C_i}{\partial X}\bigg|_{x=1} = 0 \tag{3.7}$$

3.1.1.2. Performance parameters

Performance parameters have to be defined for the complete cycle with the fractionation scheme in mind. Figure 3-1 helps with the explanation of these. Between both products originating in the reaction studied, $A + B \leftrightarrow C + D$, the most retained one is D and the least is C. The intervals for the fractionation are also listed below:

t_0 to t_1 – Desorbent is being collected;

t_1 to t_2 – Raffinate is being collected;

t_2 to t_3 – Mixture to recycle is being collected;

t_3 to t_4 – Extract is being collected (t_4 is also the time that the new feed step can start).

Figure 3-1 – Fixed Bed Chromatographic Reactor with possible fractionation scheme for reaction of type $\boldsymbol{A + B \leftrightarrow C + D}$ with less (C) and more (D) adsorbed species as raffinate and extract respectively. D-desorbent, F-feed, R-raffinate, X-extract.

Raffinate Purity is defined as the quantity of product C that leaves the bed between t_1 and t_2 relatively to all species that exit at the same time interval given by equation (3.8) (basis without solvent).

$$PuR(\%) = \frac{Q_R \int_{t_1}^{t_2} C_{C,R}\,dt}{Q_R \int_{t_1}^{t_2} (C_{B,R} + C_{C,R} + C_{D,R})\,dt} \times 100 \tag{3.8}$$

Extract Purity is defined by the quantity of product D that leaves the bed between t_3 and t_4 relatively to all species that exit at the same time interval given by equation (3.9) (basis without solvent).

$$PuX(\%) = \frac{Q_X \int_{t_3}^{t_4} C_{D,X}\,dt}{Q_X \int_{t_3}^{t_4} (C_{B,X} + C_{C,X} + C_{D,X})\,dt} \times 100 \tag{3.9}$$

Conversion of Limiting Reagent B is given by the amount of product B converted (i.e., feed minus the amount collected in the raffinate and extract) as compared to the feed one, as represented by equation (3.10),

$$X_B(\%) = 100\left(1 - \frac{Q_R \int_{t_1}^{t_2} C_{B,R}\,dt + Q_X \int_{t_3}^{t_4} C_{B,X}\,dt}{Q_F \times \Delta t_{feed} \times C_{B,0}}\right) \tag{3.10}$$

Productivity of product C is given by equation (3.11).

$$PR\left(kg_C\ day^{-1} L_{ads}^{-1}\right) = \frac{Q_R \int_{t_1}^{t_2} C_{C,R}\,dt}{1000} \times \frac{MW_C}{1000} \times \frac{cycles}{day} \times \frac{1}{V_{ads}} \tag{3.11}$$

Desorbent Consumption is given by equation (3.12) and represents the total amount of desorbent A that is taken away with the raffinate and extract fraction

$$DC(L_A\ kg_C^{-1}) = \frac{Q_R \int_{t_1}^{t_2} C_{A,R}dt + Q_X \int_{t_3}^{t_4} C_{A,X}dt}{Q_R \int_{t_1}^{t_2} C_{C,R}dt} \times \frac{MW_A}{MW_C \times \rho_A} \quad (3.12)$$

In all equations above, R, X and F mean, raffinate, extract and feed, and Q_R, Q_X, Q_F are their respective flow rates.

In the time period t_1, the only component leaving the column is the desorbent (species A) since the column was previously regenerated and is saturated with desorbent. This volume can be totally recycled back to the inlet tank. At time period between t_1 and t_2 the less retained species (raffinate – species C) can be collected, and stop the collection of this species when its concentration decreases to some specified value, or when limiting reactant or more retained species start to elute. In the time interval between $t_2$and t_3 the effluent is composed of several species, so one should collect it into a reservoir for later recycle also. Between t_3 and t_4 the fraction collected should be rich in the more retained species (species D) and desorbent. This last fraction is supposed to be integrated with a purification system for desorbent separation so that it could be reused. Likewise, the fraction containing our product (raffinate) is fed to a purification system so that desorbent and main product can be recovered separately and the desorbent recovered reused once again.

When the more retained species starts to elute, the regeneration can be started. After the outlet concentration of the most retained species is below some value a new feed step can be initiated. The collection for recycle should stop and collection of the next fraction starts when the outlet is composed again of only 2 species, one being the desorbent and the other one the most retained species D (extract). During regeneration desorbent is fed until the concentration of the most retained species drops to a desired value, so that new production step can be initiated.

3.1.2. RFCR

3.1.2.1. Initial and Boundary Conditions

The main difference between the FBCR and RFCR is that there are now two columns interconnected, plus a stream entering at that same junction. A balance must be made at this junction concerning the velocities and the species passing through that point. The balances translate into the following equations (3.13) and (3.14):

$$v_{bed2} = v_{bed1} + v_{feed} \quad (3.13)$$

$$C_{i,bed2}^{in} = \frac{C_{i,bed1}^{out} v_{bed,1} + C_{i,feed} v_{feed}}{v_{bed,2}} \quad (3.14)$$

where the velocities are all interstitial velocities, v_{bed2} and v_{bed1} are interstitial velocities in bed 2 and 1, and $C_{i,bed1}^{out}$ is the concentration of species i at the outlet of the first bed, $C_{i,bed2}^{in}$ is the concentration of the species i at the inlet of the second bed. These apply only when there is feed entering the system, otherwise equations (3.15) and (3.16) apply.

$$v_{bed2} = v_{bed1} \tag{3.15}$$

$$C_{A,bed2}^{in} = C_{A,bed1}^{out} \tag{3.16}$$

In the beginning, both beds are saturated with A. At the inlet of desorbent, in the extremities, and in the middle of the RFCR, the initial conditions change only after the last reversal. During the feed period, there are two different sets of operating conditions for the first bed and second bed. The first set of conditions is given in Table 3-3.

Table 3-3 – Desorbent inlet conditions before last reversal of the RFCR.

Desorbent inlet	Feed inlet
$C_{A,0} = 17.126M$ $C_{B,0} = C_{C,0} = C_{D,0} = 0M$ $v_{sup} = 0.1\ cm\ s^{-1}$	$C_{A,0} = 7.514M$ $C_{B,0} = 7.514M$ $C_{C,0} = C_{D,0} = 0$ $v_{sup} = 0.1 cm\ s^{-1}$

At the last reversal, the conditions change so that the bed opposed to the desorbent inlet is kept at the same flow conditions, but only the desorbent inlet is active now. The second set of conditions is given in Table 3-4.

Table 3-4 – Feed inlet conditions at the last reversal of the RFCR.

Desorbent inlet	Feed inlet
$C_{A,0} = 17.126M$ $C_{B,0} = C_{C,0} = C_{D,0} = 0M$ $v_{sup} = 0.2\ cm\ s^{-1}$	$C_{A,0} = C_{B,0} = C_{C,0} = C_{D,0} = 0$ $v_i = 0\ cm\ s^{-1}$

The boundary conditions are the same as before with equations (3.6) and (3.7).

Figure 3-2, in conjunction with Figure 3-3, explain the fractionation strategy followed here. For the top left illustration in Figure 3-2, if operating under optimal conditions, until the next reversal, two fractions are collected, desorbent recycle and raffinate, seen in Figure 3-3 as the first pair of 1 and 2. After reversal takes place, the desorbent inlet was switched, top right illustration in Figure 3-2, and collection of a new desorbent recycle and raffinate fractions begins, represented in Figure 3-3 as the second pair of 1 and 2. After the last reversal, 4 fractions are collected, desorbent recycle raffinate,

mixture recycle and extract. The illustration of this last reversal is represented as the bottom scheme in Figure 3-2, and comprises the sequence 1, 2, 3 and 4 in Figure 3-3.

The dashed lines represent the path followed to the receiving tank if the system is on the last reversal or if the system needs to collect such fractions. These, mixture recycle and extract, are usually collected after the last reversal.

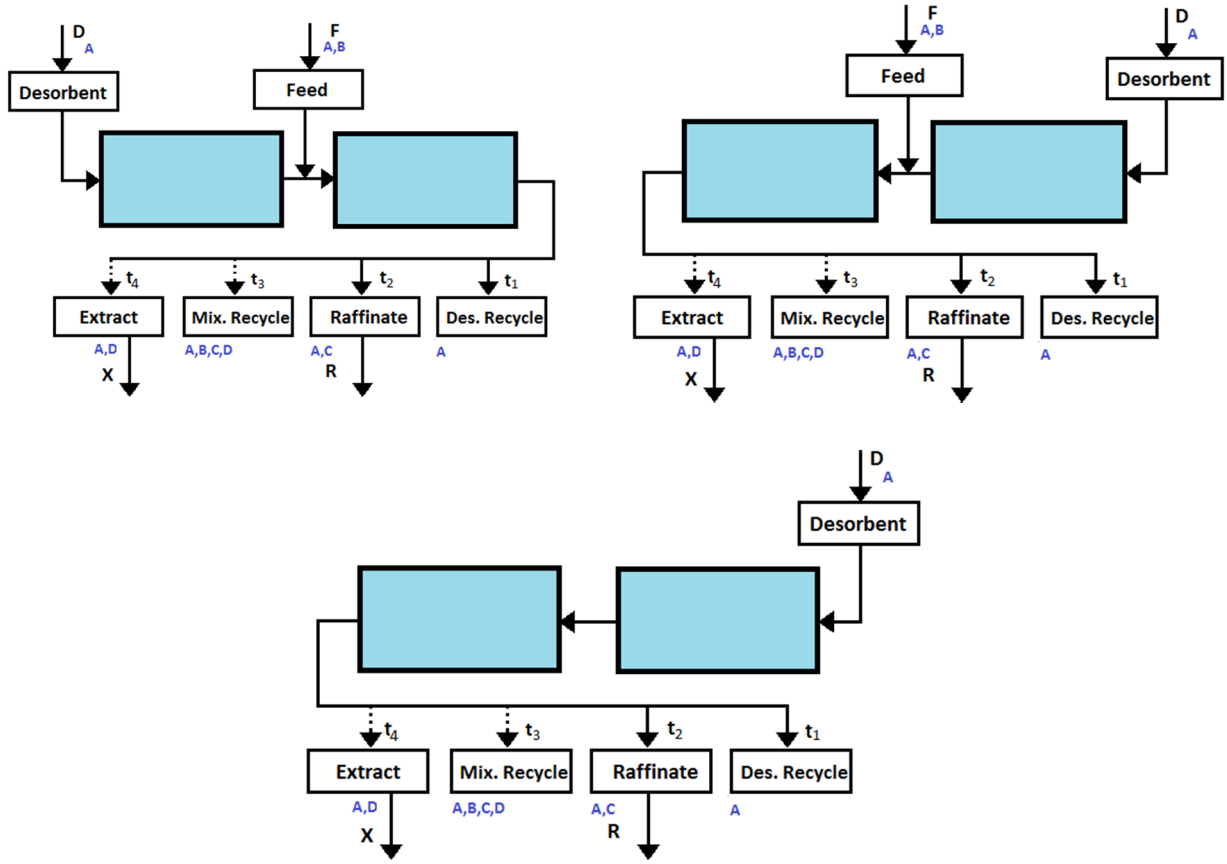

Figure 3-2 – Schemes of the RFCR as modeled. Collection scheme before (left), after (right) reversal and in regeneration mode (bottom).

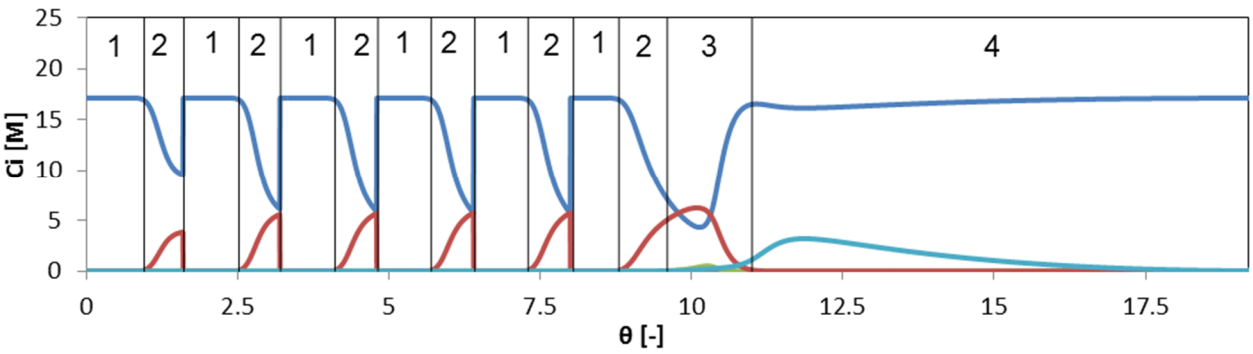

Figure 3-3 – Fractionation scheme for the RFCR outlet stream with reaction of the type $\boldsymbol{A} + \boldsymbol{B} \leftrightarrow \boldsymbol{C} + \boldsymbol{D}$. 1 – Desorbent recycle, 2 – Raffinate collection, 3- Mixture recycle, 4 – Extract Collection.

While traveling, some species will react, and the species with less affinity will elute first allowing the collection of a pure fraction of this less retained species. Just when other species start to elute, the flow is switched and the reactants will be carried to the left to the clean section of the column. After some time, the less retained species can be collected again. The less retained species travel over the more retained ones, so if this reversal operation is repeated several times, there will be an accumulation of the more retained species near the feed inlet, that ultimately will lead to a regeneration step in which the column is freed from all species except the eluent which also acts as reactant.

3.1.2.2. Performance parameters

The performance parameters are almost the same as the FBCR in section 3.1.1.2., but for raffinate and desorbent consumption the terms concerning the raffinate are substituted by a summation of all terms since with the RFCR we have several raffinate fractions in the same run. Like the FBCR we only have one extract fraction collected during one complete operation cycle.

Raffinate Purity is defined as the quantity of product C that leaves the bed in all intervals where raffinate is collected, between $t_{start,j}$ and $t_{end,j}$ relatively to all species that exit at the same time interval given by equation (3.17).

$$PuR(\%) = \frac{Q_R\left(\sum_{j=1}^{n}\left(\int_{t_{start,j}}^{t_{end,j}} C_{C,R}dt\right)\right)}{Q_R\left(\sum_{j}^{n}(\int_{t_{start,j}}^{t_{end,j}}(C_{B,R} + C_{C,R} + C_{D,R})dt)\right)} \times 100 \tag{3.17}$$

In the equation above n is the number of raffinate fractions collected.

Extract Purity is defined by the quantity of product D that leaves the bed in the last period, after the last raffinate fraction was collected. That is relative to all species that exit at the same time interval given by equation (3.18).

$$PuX(\%) = \frac{Q_X \int_{t_{start,X}}^{t_{end,X}} C_{D,X}dt}{Q_X \int_{t_{start,X}}^{t_{end,X}}(C_{B,X} + C_{C,X} + C_{D,X})dt} \times 100 \tag{3.18}$$

Conversion of Limiting Reagent B is given by the amount of product B consumed as compared to the feed one, as represented by equation (3.19),

$$X_B(\%) = 100\left(1 - \frac{\left(\sum_{j=1}^{n}\left(Q_R \int_{t_{start,j}}^{t_{end,j}} C_{B,R}dt\right) + Q_X \int_{t_3}^{t_4} C_{B,X}dt\right)}{Q_F \times \Delta t_{feed} \times C_{B,0}}\right) \tag{3.19}$$

where $\sum_{j=1}^{n}\left(Q_R\int_{t_{start,j}}^{t_{end,j}}C_{B,R}dt\right)+Q_X\int_{t_3}^{t_4}C_{B,X}dt$ represents the number of moles of B that are taken away in n fractions of raffinate plus in the extract.

Desorbent Consumption is given by equation (3.20) and represents the total amount of desorbent A that is taken away with the raffinate and extract fraction per mass unit of component C produced:

$$DC(L_A\ kg_C^{-1}) = \frac{\left(\sum_{j=1}^{n}\left(Q_R\int_{t_{start,j}}^{t_{end,j}}C_{A,R}dt\right)+Q_X\int_{t_3}^{t_4}C_{A,X}dt\right)}{\sum_{j=1}^{n}\left(Q_R\int_{t_{start,j}}^{t_{end,j}}C_{C,R}dt\right)}\times\frac{MW_A}{MW_C\times\rho_A} \tag{3.20}$$

where n represents the number of raffinate fractions collected.

Productivity is given by equation (3.21),

$$PR\left(kg_C\ day^{-1}L_{ads}^{-1}\right) = \frac{\sum_{j=1}^{n}\left(Q_R\int_{t_{start,j}}^{t_{end,j}}C_{C,R}dt\right)}{1000}\times\frac{MW_C}{1000}\times\frac{cycles}{day}\times\frac{1}{V_{ads}} \tag{3.21}$$

where n represents the number of raffinate fractions collected.

3.1.3. SMBR

3.1.3.1. Boundary Conditions

Being simulated by at least 4 FBCR models (one per zone), this concept needs more balances in all the interconnections or nodes. The velocities at the nodes are determined by the equations (3.22), (3.23), (3.24) and (3.25).

$$v_I = v_{IV} + v_D \tag{3.22}$$

$$v_{II} = v_I - v_X \tag{3.23}$$

$$v_{III} = v_{II} + v_F \tag{3.24}$$

$$v_{IV} = v_{III} - v_R \tag{3.25}$$

The subscripts I, II, III and IV are for the interstitial velocities in the respective bed sections in Figure 2-6; the subscripts D, X, F and R stand for desorbent, extract, feed and raffinate and are also related to their respective fluid velocities.

Since the natures of the streams entering the system are all different, the concentrations are given by the equations (3.26), (3.27), (3.28) and (3.29),

$$C_{i,I}^{in} = \frac{C_{i,IV}^{out}v_{IV} + C_{i,D}v_D}{v_I} \tag{3.26}$$

$$C_{i,II}^{in} = C_{i,I}^{out} \tag{3.27}$$

$$C_{i,III}^{in} = \frac{C_{i,II}^{out} v_{II} + C_{i,F} v_F}{v_{III}} \quad (3.28)$$

$$C_{i,IV}^{in} = C_{i,III}^{out} \quad (3.29)$$

which are extended to all components.

3.1.3.2. Performance Parameters

Although the performance parameters for this type of reactor are the same as before, except that these are continuous currents, they were not studied.

3.2. Simulation

Solving a PDE is not a straightforward operation. If the PDE is simple, even an analytical solution can be written; if not its solution can often be approximated by series of terms or computed numerically. When solving a system of PDE's the solutions are not always easy to compute and numerical methods come into play. Even for some specific types of problems (i.e. stiffness) the numerical methods are not accurate and attention should be paid to which methods work best for each type of problem that may be presented. Dedicated solvers can be built but usually engineers resort to ready-made solutions in order to reduce development time.

Several numerical tools became available over the years. Some are proprietary like MATLAB and gPROMS and others can be used under the General Public License. These have already powerful algorithmic tools incorporated that were perfected over the years and sometimes in conjunction with clients (that want to have tools for specific problems). The advantages of using a software tool are clear, like less time spent on debugging code and more time experimenting new concepts.

Other alternatives used previously to simulate reactive chromatography include general solvers like gPROMS and FORTRAN routines packages like PDECOL and BACOLR. gPROMS uses orthogonal collocation on finite elements (OCFEM) while MATLAB solver uses Finite Differences (FDM). On all of these tools the user can develop its own models and its own numerical methods from the ground. The objective of this thesis was to use MATLAB® as development tool.

The simulations were performed on an Intel i5 computer with 32-bit MATLAB® installation. Different types of chromatographic reactors are simulated.

3.2.1. Implementation in MATLAB® using "*pdepe*" solver

The MATLAB® intrinsic PDE numerical tool *pdepe* was used. This numerical tool proved to be very flexible for the implementation of all the concepts proposed.

The PDEs provided should be in the format of equation (3.30),

$$\boldsymbol{c}\left(\boldsymbol{x},\boldsymbol{t},\boldsymbol{u},\frac{\boldsymbol{\partial u}}{\boldsymbol{\partial x}}\right)\frac{\boldsymbol{\partial u}}{\boldsymbol{\partial t}} = \boldsymbol{x}^{-\boldsymbol{m}}\frac{\boldsymbol{\partial}}{\boldsymbol{\partial x}}\left(\boldsymbol{x}^{\boldsymbol{m}}\boldsymbol{f}\left(\boldsymbol{x},\boldsymbol{t},\boldsymbol{u},\frac{\boldsymbol{\partial u}}{\boldsymbol{\partial x}}\right)\right) + \boldsymbol{s}\left(\boldsymbol{x},\boldsymbol{t},\boldsymbol{u},\frac{\boldsymbol{\partial u}}{\boldsymbol{\partial x}}\right) \tag{3.30}$$

in which the inputs are c, f, s, coefficients of the PDE. f is a flux term and s is a sink or source term, while c is another coefficient relating to time. For cases in which there is no reaction or adsorption, the source term s is set to zero. m is a parameter to indicate slab, cylindrical or spherical geometry.

As a simple example, for just one PDE describing convection and dispersion in axial direction, if we provide

$$c = 1$$
$$f = -c_A + \frac{1}{\mathrm{Pe}}\frac{\partial c_A}{\partial x}$$
$$s = 0$$

the PDE being solved would be the convection diffusion equation, equation (3.31).

$$\frac{\partial c_A}{\partial \theta} = \frac{1}{\mathrm{Pe}}\frac{\partial^2 c_A}{\partial x^2} - \frac{\partial c_A}{\partial x} \tag{3.31}$$

This equation is used below in section 3.2.2., to assess the error of this tool in a dispersive non-reactive system.

The vectors c, f and s should be provided as separate *m-files*, although nested functions can be created to keep files organized.

Boundary conditions take the form of equation (3.32).

$$p(x,t,u) + q(x,t) \times f\left(x,t,u,\frac{\partial u}{\partial x}\right) = 0 \tag{3.32}$$

in which $p(x,t,u)$ and $q(x,t)$ are vectors for systems of PDEs.

The Danckwerts' boundary conditions are equations (3.33) and (3.34).

$$v_{int}c_{A0} = v_{int}c_A - D_{ap}\frac{\partial c_A}{\partial z}\ for\ z = 0 \tag{3.33}$$

$$\left.\frac{\partial c_A}{\partial x}\right|_{z=L} = 0 \tag{3.34}$$

In dimensionless form (except concentration) with $x = z/L$ and $\mathrm{Pe} = \frac{v_{int}L}{D_{ap}}$, the equations (3.35) and (3.36) are obtained.

$$c_{A0}|_{x=0} = c_A - \frac{1}{\mathrm{Pe}} \frac{\partial c_A}{\partial x} \tag{3.35}$$

$$\left.\frac{\partial c_A}{\partial x}\right|_{x=1} = 0 \tag{3.36}$$

So, in order to input boundary conditions of this type set $ql = 1$ and $pl = c_{A0}$ and we would construct a statement like equation (3.37).

$$\boldsymbol{c_{A0} + 1 \times \left(-c_A + \frac{1}{\mathrm{Pe}} \frac{\partial c_A}{\partial X}\right) = 0} \leftrightarrow \boxed{c_{A0} = c_A - \frac{1}{\mathrm{Pe}} \frac{\partial c_A}{\partial X}} \tag{3.37}$$

This is one of the Danckwerts boundary conditions. Similarly, for the right boundary condition, setting $qr = 1$ and $pr = c_A$ we get equation (3.38).

$$c_A + 1 \times \left(-c_A + \frac{1}{\mathrm{Pe}} \frac{\partial c_A}{\partial X}\right) = 0 \leftrightarrow c_A - c_A + \frac{1}{\mathrm{Pe}} \frac{\partial c_A}{\partial X} = 0 \leftrightarrow \boxed{\frac{\partial c_A}{\partial X} = 0} \tag{3.38}$$

3.2.2. Validation of Simulation tool

In order to assess *pdepe* conservative properties, *tracer experiments* should be performed. A pulse injection was introduced to the system and the balance between amount injected and collected is compared. Also, a reactive mixture was fed and the amount of mass unreacted and reacted was compared.

Tracer Experiment Simulation

For the non-reactive system, a pulse injection was performed during $\Delta\theta = 0.05$ ($\Delta t = \Delta\theta\tau$). The reaction term is not present and the behavior observed is a wave of solute traveling along the column as presented in Figure 3-4. The injection pulse was dispersed along the column as expected. The simulation was given enough time for the material to leave completely the column.

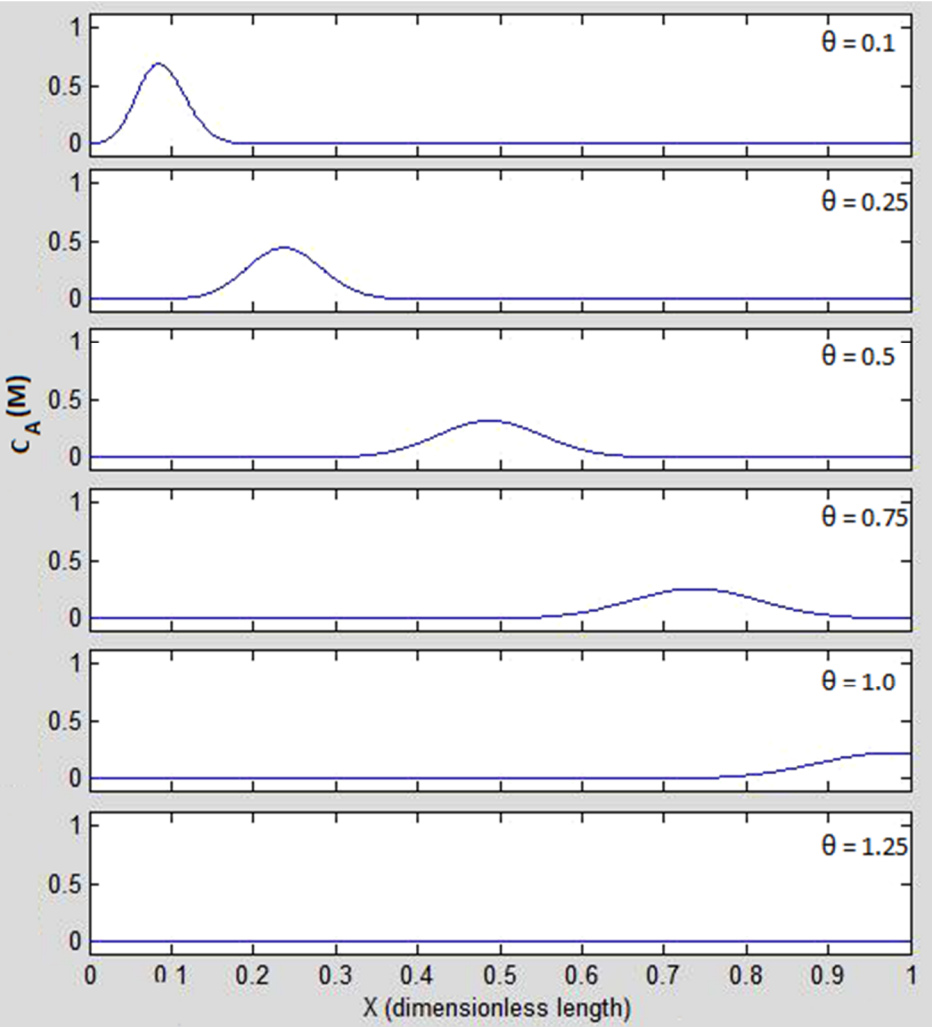

Figure 3-4 – Evolution of the concentration profile along the column for different $\boldsymbol{\theta}$, Pe=250.

Assuming that Q is constant, the amount of material injected is simply given by equation (3.39),

$$n_A^{in} = Q C_A \Delta t \tag{3.39}$$

and the amount of material collected given by equation (3.40).

$$\boldsymbol{n_A^{out} = Q \int_0^t C_A dt} \tag{3.40}$$

So the error is given by equation (3.41).

$$\boldsymbol{E}[\%] = \frac{\boldsymbol{n_A^{in} - n_A^{out}}}{\boldsymbol{n_A^{in}}} \times \mathbf{100} = \left(1 - \frac{\int_0^{\theta} \boldsymbol{C_A d\theta}}{\boldsymbol{C_A \Delta \theta}}\right) \times \mathbf{100} \tag{3.41}$$

The results for the conditions herein employed are provided in Table 3-5. The magnitude of the error is very low given the amount of material that is injected and is collected at the outlet.

Table 3-5 - Mass balance simulation error (tracer experiment).

$n_A^{in}\ [mol]$	$n_A^{out}\ [mol]$	E [%]
2.654	≈2.654	0.0006 %

Reactive Chromatography Simulation ($A \leftrightarrow B + C$)

The conservative properties of the tool were also quantified for a reaction of the type $A \leftrightarrow B + C$. The number of moles of A injected should give origin, at the outlet, if all A reacts, to two times the moles injected since it is a dissociative reaction. In this case, the solvent interaction was not considered. The species are transported by a flow of inert fluid.

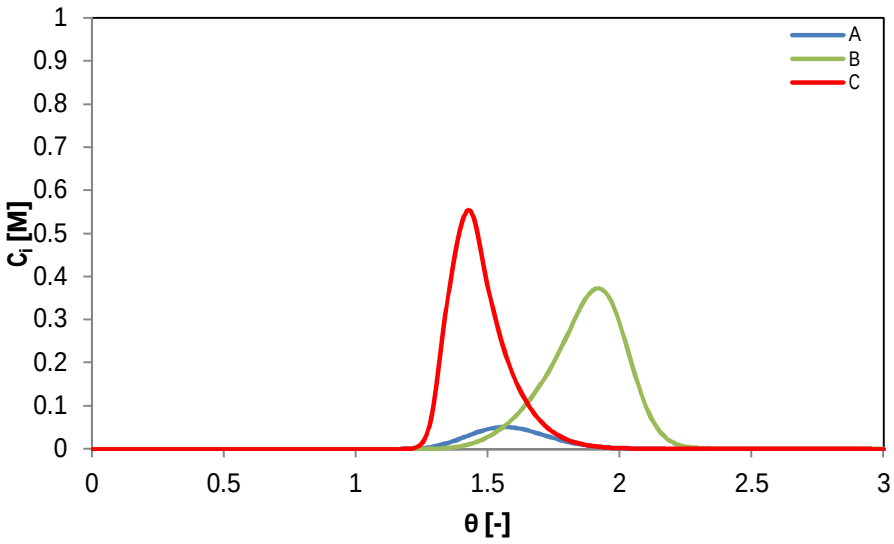

Figure 3-5 – Outlet concentration profiles for the test injection with reaction of the type $A \leftrightarrow B + C$. Affinity towards the adsorbent is in the order $K_C<K_A<K_B$.

An injection of duration $\Delta\theta$ = 0.15 ($\Delta t = \Delta\theta\tau$) was introduced. The concentration for the duration of injection was constant at C_A = 1.0 M. The amount of material injected and collected was compared using the outputted data of the run (Figure 3-5). The error was calculated according to the formula below, equation (3.43).

The amount of material injected is again given by equation (3.39), and the amount of A detected at the outlet is also given by equation (3.40), but now, the material injected should give origin to twice the number of moles injected. So the amount of material B and C collected is evaluated with equation (3.42).

$$n_B^{out} + n_C^{out} = Q \int_0^t (C_B + C_C)dt \qquad (3.42)$$

The error is given by equation (3.43)

$$
\begin{aligned}
E[\%] &= \frac{2\left(n_A^{in} - n_A^{out}\right) - \left(n_B^{out} + n_C^{out}\right)}{2\left(n_A^{in} - n_A^{out}\right)} \times 100 \\
&= \frac{2\left(QC_A\Delta t - Q\int_0^t C_A dt\right) - Q\int_0^t (C_B + C_C)dt}{2\left(QC_A\Delta t - Q\int_0^t C_A dt\right)} \\
&= \left(1 - \frac{\int_0^{\theta_{end}} (C_A + C_B)d\theta}{2\left(C_A\Delta\theta - \int_0^{\theta_{end}} C_A d\theta\right)}\right) \times 100
\end{aligned}
\tag{3.43}
$$

$2\left(n_A^{in} - n_A^{out}\right)$ represents the number of moles that should have originated from the amount of A reacted. As seen in the Figure 3-5, the reaction was not complete therefore $n_A^{out} \neq 0$. The resulting error is quantified in Table 3-6.

Table 3-6 – Mass balance simulation error (reactive chromatography).

$n_A^{in}\ [mol]$	$n_A^{out}\ [mol]$	$n_B^{out} + n_C^{out}\ [mol]$	$E\ [\%]$
7.964	1.008	13.846	0.5 %

If the numerical methods behind *pdepe* were truly conservative, the error would have been lower. Specialized numerical tools designed to deal with physical phenomena tend to have smaller errors.

4. Results and Discussion

In this chapter, for the equilibrium dispersive model, the effect of the kinetic constant, separation factor and switch time (only for the RFCR) will be studied through several performance parameters defined in previous chapter for different chromatographic reactors. For that, simulations were made on which only the parameter to be studied is changed. All other parameters like Pe, τ were kept the same. The simulations were performed for the reaction type $A + B \leftrightarrow C + D$ in which A also serves as desorbent. The equilibrium constant is also the same, $K_{eq} = 1.4$.

Results of simulations were analyzed in terms of productivity (amount of product C collected per adsorbent volume per day) and desorbent consumption (amount of desorbent A spent per amount of product C obtained), reactant B conversion, and purities of raffinate and extract fractions. Performance parameters used were defined in the modeling section of the respective chromatographic reactor (cf. chapter 3). In the case of RFCR, all of the performance parameters with the exception of PuX have to take into account the several fractions of Raffinate. Obtaining high purity fractions was the main goal. The regeneration step lasts until the concentration of species A returns to its initial concentration of 17.126 M inside the reactor. A comparative resume of the FBCR and RFCR is made in the last section.

4.1. FBCR Results

A resume of working conditions simulated for the FBCR is presented in Table 4-1. In reality, for each run presented, at least 4 runs were made in order to confirm the convergence of the recycled feed composition but, more importantly, the convergence of performance parameters. The reference case, run #1, is presented next for a better understanding.

Table 4-1 – FBCR run parameters resume.

Run	$\Delta\theta_{feed}[-]$	$\theta_{run}[-]$	$\tau\ [s]$	Pe $[-]$	$k'\ [M^{-1}s^{-1}]$	$d\theta\ [-]$	$\alpha_{DC}[-]$
#1	1.6	8.64	50	125	0.01	0.01	3.88
#2	1.67	8.73					3
#3	1.6	8.66					2.35
#4	1.6	8.96					2
#5	1.6	8.69			0.02		3.88
#6	0.80	7.73			0.001		3.88

$\Delta\theta_{feed}$ is the duration of feed, and θ_{run} is the end of the run (total duration) until complete regeneration, τ is the holdup time, Pe is the Peclet number, k' is the kinetic constant, $d\theta$ was the time step and α_{DC} is the separation factor. The separation factor can be defined in terms of a ratio of the isotherm parameters $K_{L,i}$:

$$\alpha_{DC} = \frac{K_{L,D}}{K_{L,C}}$$

with C being the less retained species and D the more.

The performance parameters of run #6 were obtained under a different duration of feed (and slightly different duration of run) because the feed duration of $\Delta\theta = 1.6$ was too large compared to the low reaction rate. A small amount of C was being formed but since in each run the stoichiometry of the mixture recycled was being adjusted adding A and / or B, the requirements of these to attain an equimolar mixture were always increasing, thus the volume to be fed in each simulation for this run was not stabilizing.

For the first simulation of run #1, species profiles are presented in Figure 4-1. The vertical lines mark the fractionation zones of the eluant (stream that leaves the column) like previously shown in Figure 2-3. At these time points, the collection vase is shifted allowing the collection of several fractions which are rich in specific components. The fraction collected between $\theta = 0$ and $\theta = 0.95$, is composed of species A only, so according to Figure 3-1, it is recycled as reusable desorbent back to the respective tank. The fraction collected between $\theta = 0.95$ and $\theta = 1.68$ constitutes the raffinate. The fraction collected between $\theta = 3.10$ and $\theta = 8.59$ is the extract. The mixture collected between $\theta = 1.68$ and $\theta = 3.10$, is the mixture to be recycled. Containing A, B, C and D, this fraction is then adjusted, so that the reactants entering the FBCR in the next run are in stoichiometric proportions. This is done adding A and/or B. For this the MS Excel Solver was used to calculate the right number of moles of each reactant (see Appendix, section "Matching stoichiometry in the mixture Recycle to feed again - FBCR").

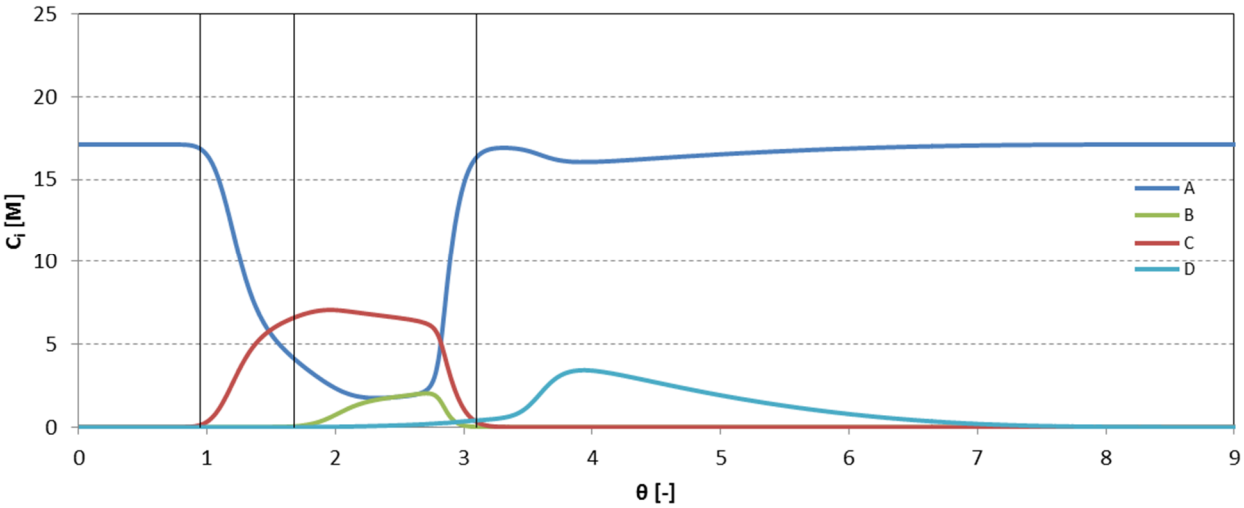

Figure 4-1 –Evolution of Simulated Eluant Concentration History (1st simulation for run #1), with fractionation scheme represented as vertical lines.

Initially the FBCR was saturated with A, and then, it starts being fed with $C_A = C_B = 7.514\ M$ which constitutes an equimolar mixture, for an interval of $\Delta\theta = 1.6$. Due to the presence of the adsorbent, the more retained species D travels slow, while the less retained species C is dragged away quickly. Also, the most retained species D, a product, is collected during the regeneration step. So it is

expected to collect C and D rich fractions that will be purified /separated from the solvent in a later stage. For these concentrations, a simple fixed bed with only catalyst would have a maximum conversion of ≈ 54% (see Appendix, section "Conversion on equilibrium (catalyst only)") and it would be impossible to collect pure fractions (in solvent free basis). Performance parameters for Figure 4-1, including conversion, are presented in Table 4-2. The conversion is very high due to the fact that no B leaves the system as raffinate or extract given their respective high purities.

Table 4-2 – Performance parameters obtained with profiles in Figure 4-1.

PR [$kg_C\ day^{-1}\ L_{ads}^{-1}$]	35.23
DC [$L_{des}\ kg_C^{-1}$]	1.76
PuR [%]	99.84%
PuX [%]	99.59%
X_B [%]	99.96%

Before a new feed is injected, a regeneration step is made with pure species A which has a concentration of 17.126 M. Then the next feed period has to be of the same duration so that the feed composition approximates the same values with time, as well as performance parameters.

For the FBCR, the duration of all the feeds was $\Delta\theta_{feed} = 1.6$ (or $\Delta t_{feed} = \theta\tau$). The profiles that follow the first simulation of run #1, Figure 4-1, for the same set of simulation parameters are very much alike the one in Figure 4-2.

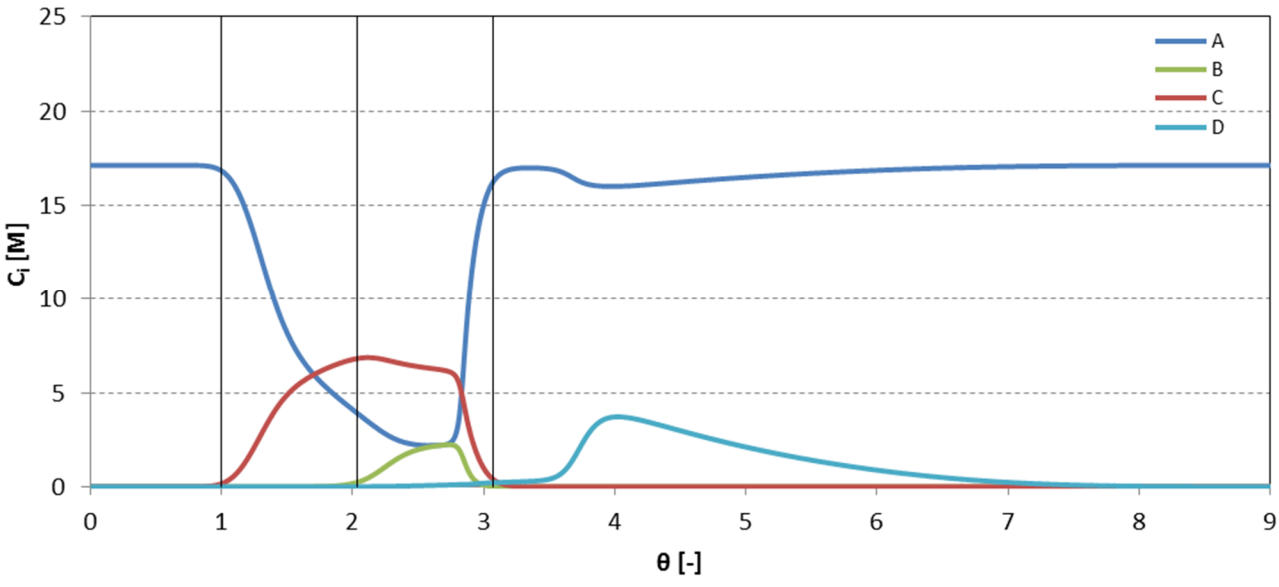

Figure 4-2 – Evolution of Simulated Eluant Concentration History (5th simulation for run #1), with fractionation scheme represented as vertical lines.

The performance parameters resulting from the last simulation (5th) for the run #1 are given in Table 4-3. These are not significantly different from the first run.

Table 4-3 – Performance parameters obtained with profiles of Figure 4-2.

PR [kg day^{-1} L_{ads}^{-1}]	34.02
DC [L_{des} kg_C^{-1}]	1.95
PuR [%]	99.77%
PuX [%]	99.61%
X_B [%]	99.93%

For dynamic simulations like these, the convergence of these values and the consistency of consecutive outlet profiles indicate that the Cyclic Steady State was reached. The performance parameters sequence is given for all simulations for run #1 in Table 4-4. Performance parameters for the other runs in Table 4-1 are given in the Appendix, from Table A-1 to Table A-5. It is clear that, although the parameters do not converge fully with only five simulations, they fluctuate around the same values.

Table 4-4 – Performance parameters convergence for run #1 with several simulations.

run #1 simulations	**1**	**2**	**3**	**4**	**5**
PR [kg_C day^{-1} L_{ads}^{-1}]	35.23	28.39	32.76	32.60	34.02
DC [L_{des} kg_C^{-1}]	1.76	2.20	1.90	2.05	1.95
PuR	99.84%	99.68%	99.79%	99.75%	99.77%
PuX	99.65%	99.56%	99.59%	99.58%	99.61%
X_B	99.96%	99.88%	99.94%	99.92%	99.93%

An illustration of the dynamic behavior of the FBCR is shown in Figure 4-3. Right after the mixture containing A and B starts being fed (θ = 0.2), a decrease of A near the inlet can be seen. In the illustration for θ = 1 the species C has already reached the outlet of the reactor. For θ = 1.6, and at $x \approx 0.3$ (dimensionless length), a plateau with constant concentrations of all intervening species just formed, it should not be allowed to continue to extend until the outlet, since this would be unproductive, that is why at this point in time, the regeneration starts. At θ = 1.7 the regeneration is already taking place, the increase in concentration of A is visible, mainly in the reactor section close to the entrance. While regenerating the bed, the most retained species, D, is clearly the last to elute. The regeneration is complete for θ = 8.64.

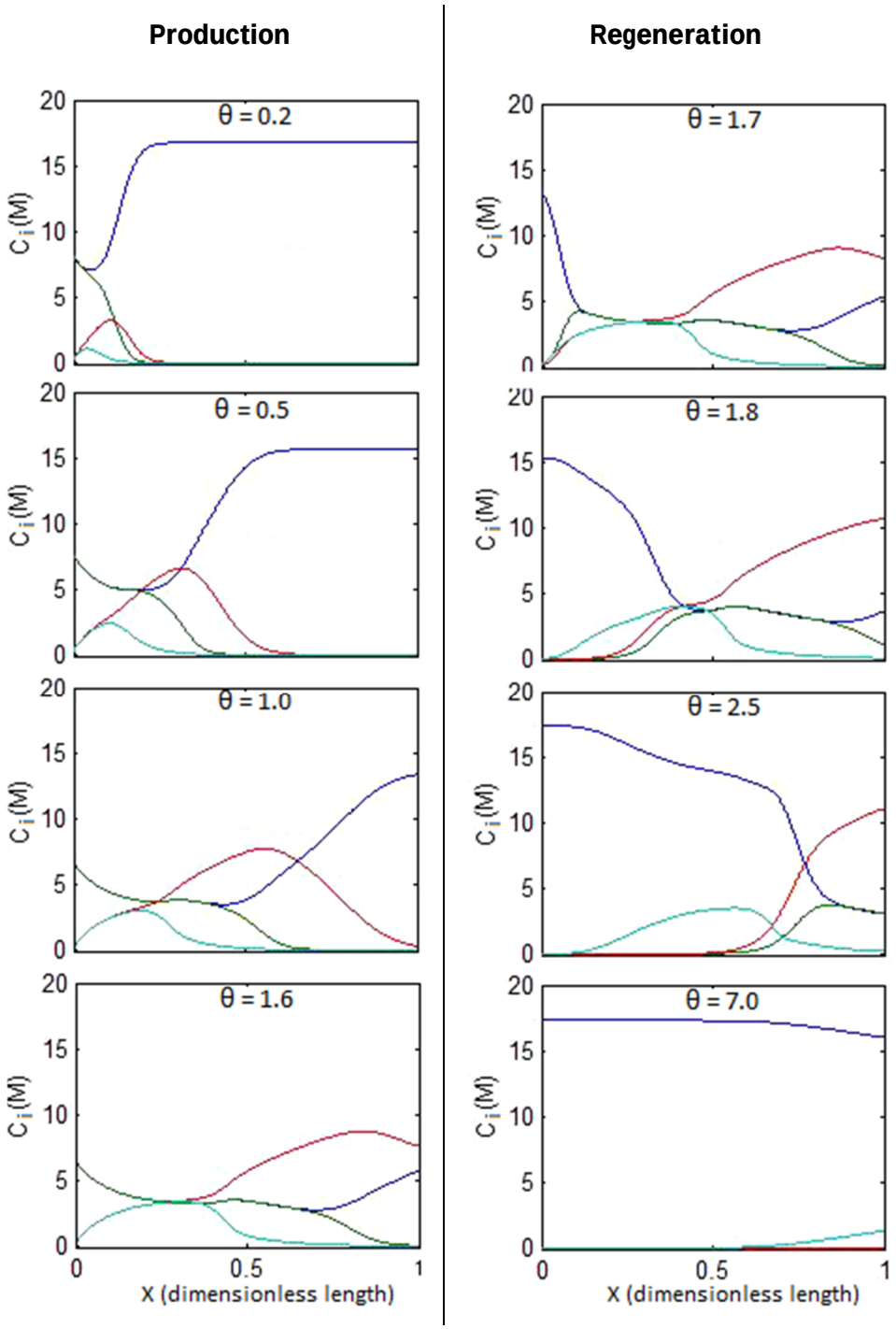

Figure 4-3 – Dynamic behavior of the FBCR during a complete cycle (production + regeneration). k'=0.01 $M^{-1}s^{-1}$. Reaction $\boldsymbol{A} + \boldsymbol{B} \leftrightarrow \boldsymbol{C} + \boldsymbol{D}$. (blue) A, (green) B, (red) C and (light blue) D. Initially the bed is saturated with A and then an equimolar feed of A + B is initiated. Later (θ > 1.6) the feed is switched to pure A for regeneration.

Influence of Kinetic Constant

The runs used to assess the role of the kinetic constant were the #1, #5 and #6 (cf. Table 4.1). The variation of the kinetic constant can be interpreted as a trial of different catalysts, and depending on the characteristics of the catalyst used, the performance of the chromatographic reactor can be enhanced.

In Figure 4-4 we can see that for successive lower orders of magnitude of the kinetic constant gives worse results for productivity and desorbent consumption as expected. Lower values of the kinetic constant do not allow the formation of products in quantities enough to significantly be pushed away from the reaction zone, thus inhibiting the dislocation of the equilibrium.

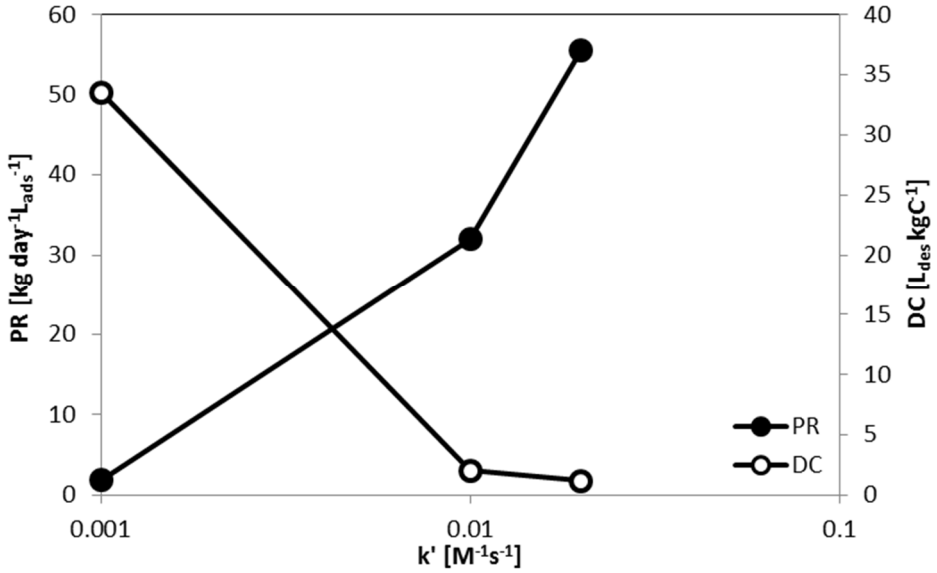

Figure 4-4 – FBCR performance parameters as function of the kinetic constant. Points for runs #1, #5 and #6.

In Figure 4-5 we can see the effect of the kinetic constant on the performance parameters purity of raffinate and conversion of species B. For high values of the kinetic constant it is possible to obtain high purity products and also high conversion of the reagent. For the highest kinetic constant both purity parameters and conversion are above 99%. This is not surprising since fractionation points (or fractions collected) are adjusted for each kinetic constant (i.e. for a higher kinetic constant the interval during which raffinate is collected can be extended, as for lower kinetic constants it is shorter). The consequence for this adjustment, in the case of lower kinetic constants, is that the volume to be recycled gets higher and higher; for the highest kinetic constant the volume recycled is 43 cm^3 as for the lowest it is 262 cm^3; clearly lowering productivity.

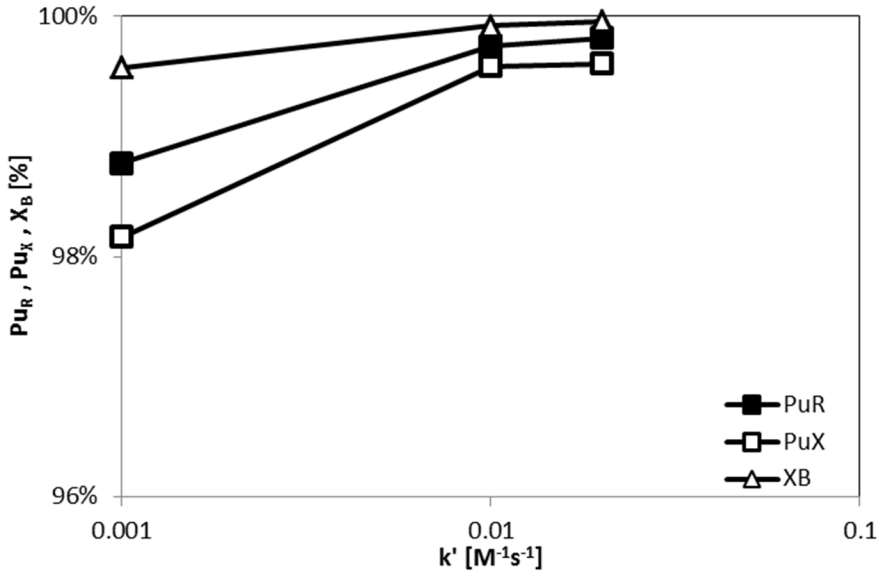

Figure 4-5 – FBCR Purities and Conversion as function of the kinetic constant. Points for runs #1, #5 and #6.

Influence of Separation Factor

If two species have a high separating factor, α_{DC}, they are easily separated, if not, the separation will be more expensive in terms of desorbent spent. Several runs were made with the intent of checking the influence of the separation factor in performance parameters. It is expected to see a decrease in the output of main product C as the separation gets harder i.e. low separating factor. Compared to the other components of the system studied, the only component having a large difference in affinity towards the adsorbent is D. The regeneration takes long because of this component.

As can be seen from the Figure 4-6 below, if the separation factor of the components is lower it becomes more difficult for the FBCR to separate the mixtures while maintaining low desorbent consumption. With a larger separation factor, species C is less retained than D and so the former travels faster along the column leaving space for new material to be converted, dislocating the equilibrium locally. This is what drives the increased productivity at higher separation factors.

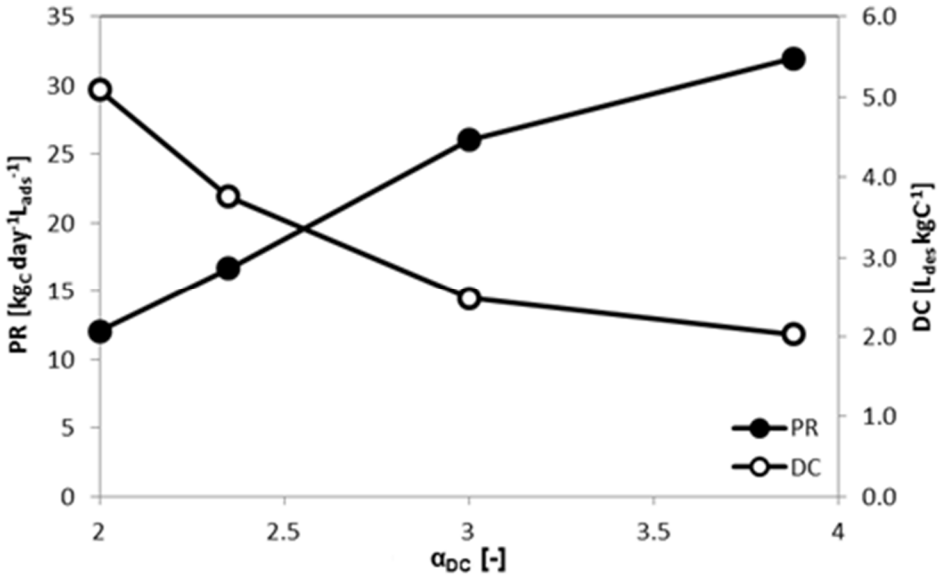

Figure 4-6 – FBCR productivity and desorbent consumption as functions of separation factor. Data for runs #1, #2, #3 and #4.

The separation between products can be greatly enhanced if the adsorbent/catalyst used does not have affinity (or at least it is much lower) towards one of the products. And the regeneration can be shortened if the regeneration step is performed at higher flows of eluent; alternatively, a specific desorbent can be fed or the conditions of the bed are altered like temperature.

Figure 4-7 presents the influence of the separating factor on achieved purities of raffinate and extract as well as conversion of reagent. This figure shows that although the separation factor has decreased significantly, the raffinate and extracts collected are still very pure. Also, conversion is very high. If we juxtapose Figure 4-6 and Figure 4-7, the cost for this is clear. The separation can still be good to collect high purity fractions but not enough to collect long fractions of this product reducing overall productivity.

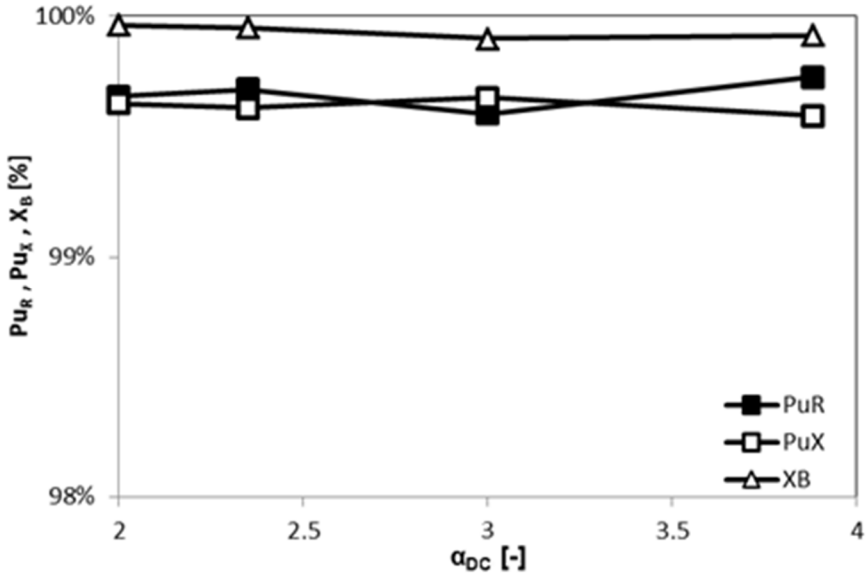

Figure 4-7 – FBCR Purities and Conversion as function of separation factor. Data for runs #1, #2, #3 and #4.

Fractions collected are beneficially manipulated. The collection of raffinate is then smaller and smaller with successive smaller values of the separation factor. The conversion is kept high because the fraction containing almost all the B not reacted is fed again.

4.2. RFCR Results

The mode of operation of the Reverse Flow Chromatographic Reactor (RFCR) is better explained with the following Figure 4-8, which gives a general idea of the dynamical behavior of this type of reactor. In the beginning, depicted by the pair of figures surrounding **a)**, both beds are saturated with A; the effect of the inlet in the middle causes a dilution of the species A and a new species B appearing, as well as small concentrations of C and D. After letting the RFCR run for a while, **b)**, the products C and D are now seen more clearly. At **c)**, the product C already reached the outlet of the column in the right and is being collected. At **d)**, the flow was reversed and we can see the concentration of A increasing on the right side/right column. In **e)** and **f)** it is clear that the wave of product C is travelling faster over the more retained ones, D. At **g)** the product C has reached the end of the column, and gets collected for a while and the flow is about to be reversed again, which can be seen in **h)**. This sequence represents the first cycle because the column on the left returned to its initial state; profiles are similar for the column on the right at **a)** and at **h)**.

It should be kept in mind that there is an equimolar feed of A and B in the middle of the two columns (or graphics). The red arrows indicate the direction of the flow at that time.

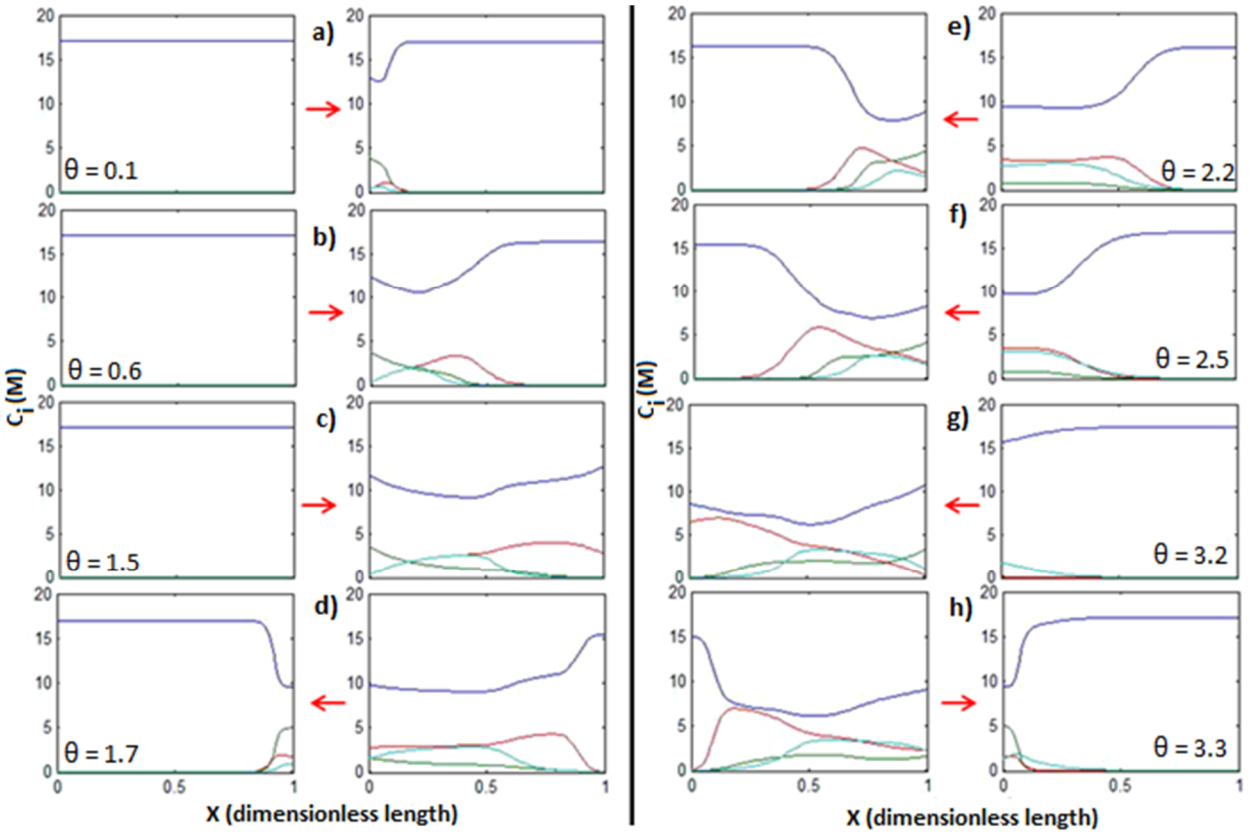

Figure 4-8 – Depiction of the dynamic behavior of the RFCR during one complete initial cycle. Reaction $\boldsymbol{A} + \boldsymbol{B} \leftrightarrow \boldsymbol{C} + \boldsymbol{D}$. (blue) A, (green) B, (red) C and (light blue) D. k'=0.01 $M^{-1}s^{-1}$.

The eluant collection is made on both sides in a sequential way. As the flow direction is switched, the collection side is also switched. The resulting outlet concentration is given in Figure 4-9 for 6 semi-cycles (or if preferred, the complete run with reversals plus regeneration). The performance parameters explained earlier in section 3.1.2.2. are applied in this section. The fractionation scheme for evaluation of performance is presented in Figure 4-9. With this type of reactor, RFCR, it is possible to collect several raffinate fractions, marked in the same figure as type (2). Between those, desorbent is collected as a separate fraction in order to be recycled, marked as type (1). Fraction of the type (3) constitutes the mixture recycle which may contain unreacted species B, and product D, as well as A and C. Finally fraction type (4) constitutes the extract which is rich in product D, the more retained species that travels slower in the reactor.

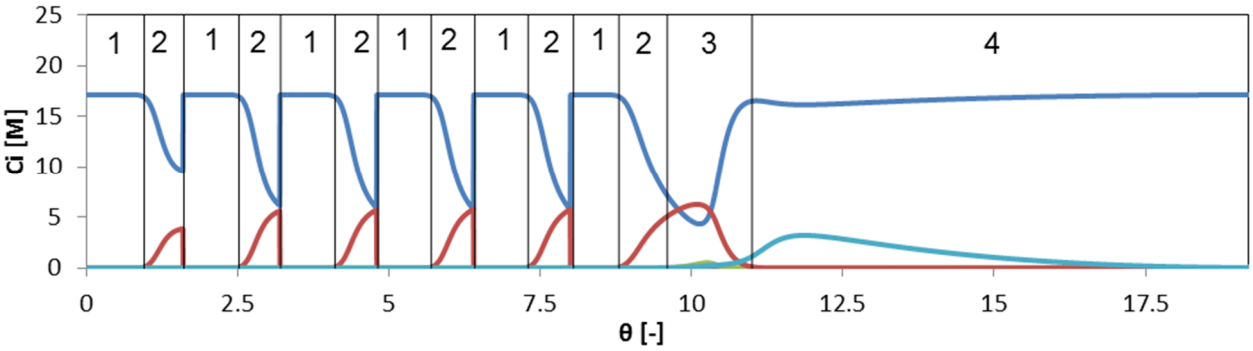

Figure 4-9 – Fractionation scheme for the RFCR outlet stream. 1 – Desorbent recycle, 2 – Raffinate collection, 3 – Mixture recycle, 4 – Extract collection. Reaction $\boldsymbol{A} + \boldsymbol{B} \leftrightarrow \boldsymbol{C} + \boldsymbol{D}$. (blue) A, (green) B, (red) C and (light blue) D. k'=0.01 $M^{-1}s^{-1}$.

The regeneration step continues after collection of the last raffinate fraction. In fact, the collection of the last raffinate fraction occurs during the regeneration step. After collecting this last raffinate fraction, the RFCR just continues to operate on the flow direction until both beds are regenerated. This procedure is done because the wave front of component D is already near the outlet. If a reversal were to take place at this moment, the product D wave would have to travel the whole 2 semi-beds again. The extra amount of desorbent spent during this unproductive semi-cycle is not worthy of reversal.

The fractionation scheme presented on Figure 4-9 was used to calculate the performance parameters. After 5 of the 6 semi-cycles the feed was switched off. The last fraction between raffinate and extract should also be returned back to the system. When the concentration on B and C is sufficiently lower than D, the extract fraction starts to be collected. The small fraction, before extract gets collected, is recycled back and also every fraction in between raffinate collections are desorbent recycling.

The parameters used in the RFCR simulations are summarized in Table 4-5. Run #1 serves as starting point for all the studies in all the simulations. The parameters τ_2 and Pe_2 reffer to the second bed to where the reaction mixture is being released and the outlet is being collected. The first bed was kept at $Pe_1 = 62.5$, $\tau_1 = 100\ s$ and reaction and adsorption parameters are the same as in the second bed.

Table 4-5 – Summary of the conditions simulated with the RFCR.

Run	$\theta_{switch}[-]$	$\theta_{run}[-]$	$\tau_2\ [s]$	Pe_2	$k'\ [M^{-1}s^{-1}]$	$d\theta\ [-]$	$\alpha_{DC}[-]$
#1	1.6	19.2	50	125	0.01	0.05	3.88
#2	1.7	20.4					
#3	1.8	21.6					
#4	2	24					
#5	1.5	18					
#6	1.4	16.8					
#7	1.6	19.2			0.001		
#8					0.02		
#9					0.1		
#10					0.01		3
#11							2.35
#12							2

Influence of Switching Time

Switch time presents an important role in cyclic operated reactors. A higher switch time means that the window for collecting our desired product C is larger, so productivity goes up as desorbent consumption goes down, as illustrated in Figure 4-10. But this increase is limited. The raffinate fraction collected starts to be impure because other species like B and D start to elute. So, increasing the switch time after some point decreases purity of raffinate and conversion of B (Figure 4-11). The purity of the extract in Figure 4-11 is unaffected because it is rich in the most retained species D, so when it elutes, in the regeneration phase, the other species are no longer present, hence the extract has always high purity.

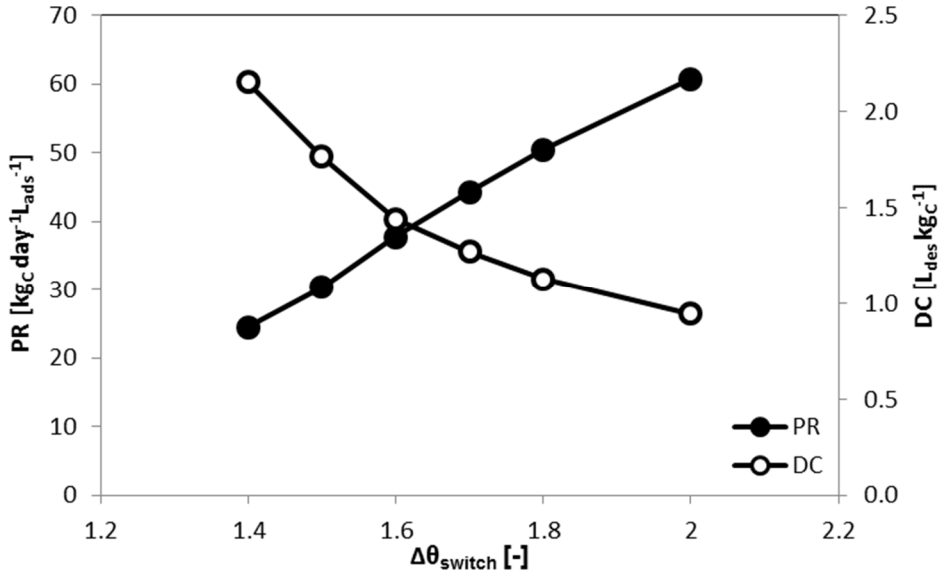

Figure 4-10 – RFCR Effect of switching times on productivity and desorbent consumption. Runs #1 to # 6.

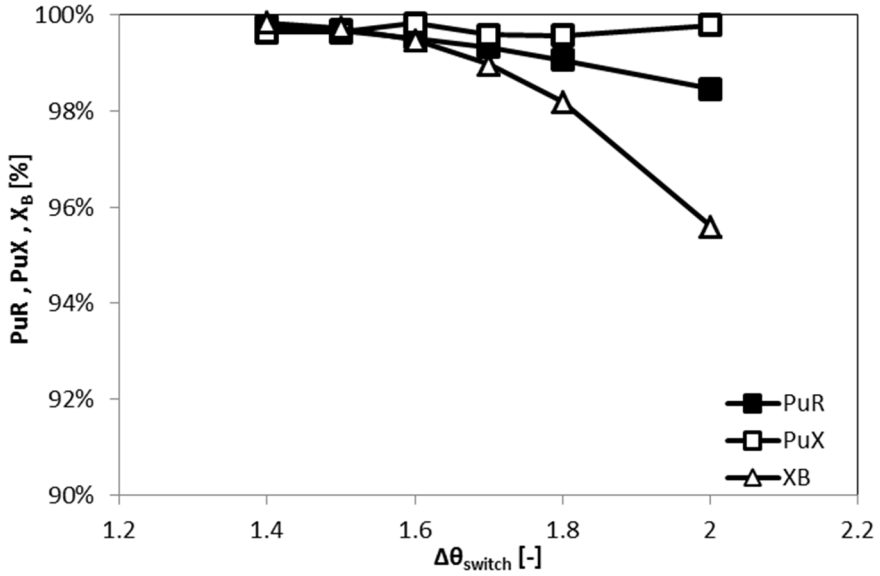

Figure 4-11 – Effect of switching times on raffinate and extract purity and conversion of B. Runs #1 to # 6.

Therefore there is an optimum switch time that maximizes productivity, conversion, purity of raffinate and at the same time decreases desorbent consumption. The optimum seems to be located around $\Delta\theta_{switch} = 1.6$. The data used to construct the two graphs above is condensed in Table 4-6.

Table 4-6 – Data for the effect of switching times on performance parameters.

$\Delta\theta_{switch}$ [-]	1.4	1.5	1.6	1.7	1.8	2
PR [$kg_C\ day^{-1}\ L_{ads}^{-1}$]	24.52	30.42	37.77	44.32	50.45	60.78
DC [L_{des}/kg_C]	2.15	1.77	1.44	1.27	1.13	0.94
PuR	99.76%	99.67%	99.52%	99.34%	99.07%	98.47%
PuX	99.63%	99.64%	99.83%	99.59%	99.57%	99.79%
X_B	99.84%	99.73%	99.48%	98.98%	98.20%	95.61%

Influence of Kinetic Constant

In general if a reaction is fast, the removal of products from the reaction medium should be facilitated. In that perspective, the results for consecutively faster reaction rates are the same as in the case of FBCR. An increase in the constant is accompanied by an increase in productivity as well as decreased desorbent consumption (Figure 4-12). Both production and desorbent consumption seem to be approximating asymptotes. From this it can be concluded that after a determined switch time is set, the increase in reaction rate will not have a significant benefit on performance parameters. So the optimum switch time varies with the reaction rate.

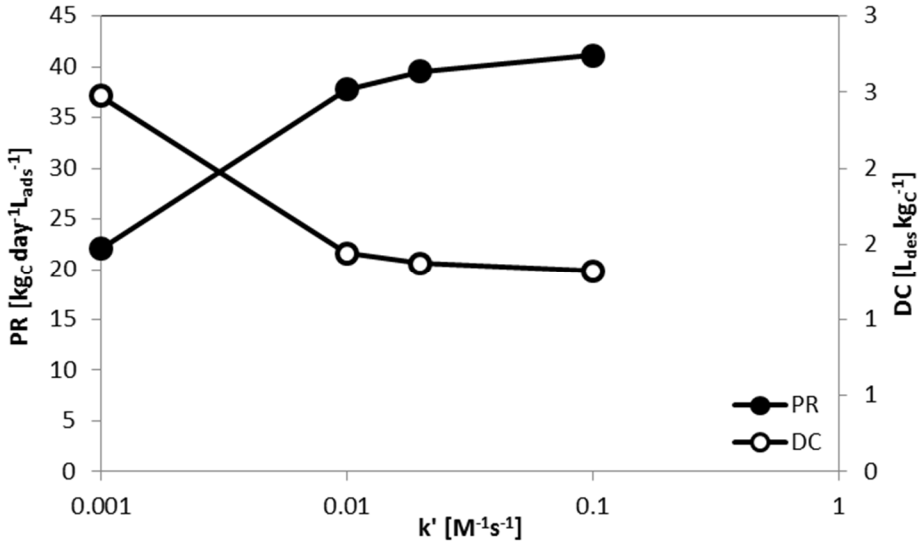

Figure 4-12 – RFCR Effect of kinetic constant on Productivity and Desorbent consumption. Runs #1, #7, #8 and #9.

For slower reactions, reagent B is not consumed before it reaches the reactor outlet, resulting in a decreased conversion and raffinate purity, as shown in Figure 4-13. The data used to obtain the graphs is presented in Table 4-7. From the data presented it is visible that for faster reactions high conversions and purities are maintained.

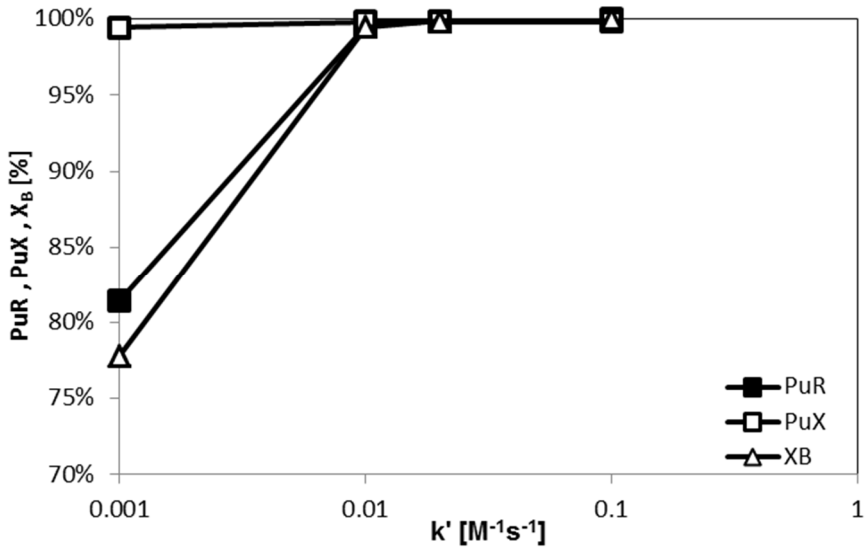

Figure 4-13 – RFCR Effect of kinetic constant on Raffinate and Extract purity and conversion of B. Runs #1, #7, #8 and #9.

Table 4-7 – RFCR Data for the effect of kinetic constant on performance parameters. Runs #1, #7, #8 and #9.

k' [$M^{-1}s^{-1}$]	0.1	0.02	0.01	0.001
PR [kg day^{-1} L_{ads}^{-1}]	41.11	39.55	37.77	22.08
DC [L_{des}/kg_{EL}]	1.32	1.37	1.44	2.48
PuR	99.99%	99.88%	99.52%	81.47%
PuX	99.83%	99.83%	99.83%	99.43%
X_B	99.98%	99.88%	99.48%	77.83%

Influence of Separation Factors

As stated before for the FBCR, the decreasing of the separating factors complicates the separation. The same is observed here. The reference point for these simulations was the run #1 with switch time of $\Delta\theta_{switch}$ = 1.6, k' = 0.01 $M^{-1}s^{-1}$, τ_2 = 50s, Pe = 125 and α_{DC} = 3.88.

For the conditions of Figure 4-14, the product C and reactant B travel with almost the same velocity and the front waves become closer with decreasing separation factor, lowering the amount of product C collected in that fixed switch time.

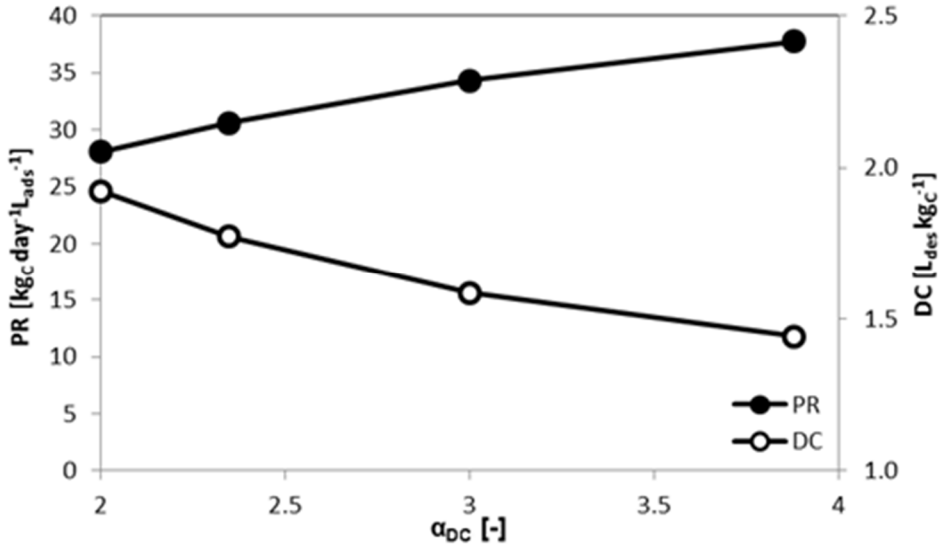

Figure 4-14 – RFCR Effect of separation factor on Productivity and Desorbent consumption. Runs #1, #10, #11 and #12.

As seen in Figure 4-15, the separation factor can be lowered but the system is still able to produce a fraction rich in C, with acceptable purities and conversion of B. Data used to produce the previous figures is provided in Table 4-8.

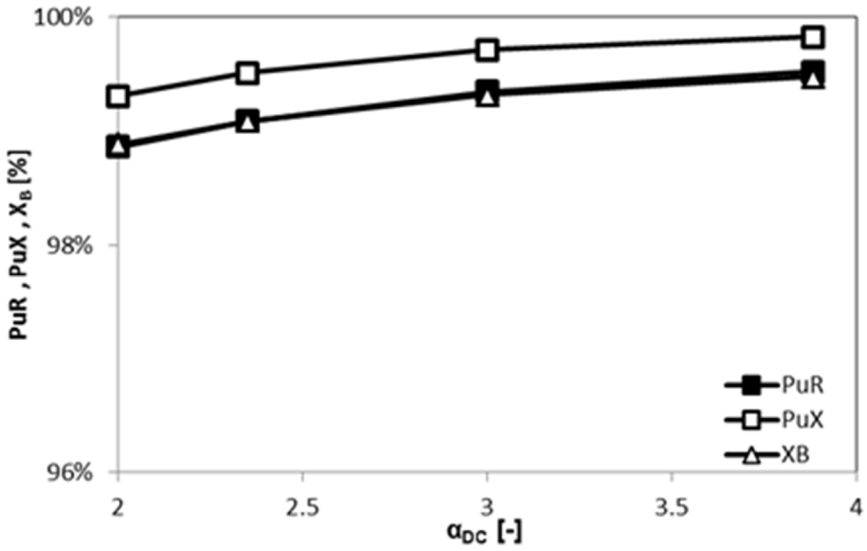

Figure 4-15 – RFCR Effect of separation factor on Raffinate and Extract purity and conversion of B. Runs #1, #10, #11 and #12.

Table 4-8 – RFCR Data for the effect of separation factor on performance parameters. Runs #1, #10, #11 and #12.

α_{DC} [-]	2	2.35	3	3.88
PR [$kg_C\ day^{-1}\ L_{ads}^{-1}$]	28.07	30.57	34.28	37.77
DC [L_{des}/kg_C]	1.92	1.77	1.59	1.44
PuR	98.86%	99.09%	99.35%	99.52%
PuX	99.31%	99.51%	99.71%	99.83%
X_B	98.89%	99.09%	99.32%	99.48%

The increased productivity can be explained in the following manner. Due to the fact that the separation factor is increased (affinities further apart), product C elutes without difficulties, or faster than D, originating a richer fraction of C. Also, if species D is less retained, the tailing in the regeneration step will not be so long, lasting less time which decreases overall working time per run, and consequently, increasing the number of runs performed in a day. In this context, during the run, the possible number of reversals is performed, including also a regeneration step. A cycle is comprised of 2 switch times (when the bed returns to the same state as before) therefore a run includes several cycles.

A major conditionality to these systems is the most retained species. Due to stronger interactions with the adsorbent material, the desorbent is not able to regenerate the bed so easily, leading to higher running times, decreasing the number of cycles that can be performed per day and the amount of desorbent necessary. Desorbent (A) consumption and cycle time could be decreased by modifying the regeneration step using a reactive desorbent that would facilitate the removal of species D (Sainio et al., 2011).

4.3. SMBR

The SMBR concept was also studied. Due to limitations of time, the optimization of the SMBR was not conducted properly. That is why only a qualitative evaluation of the SMBR simulation can be made. Figure 4-16 presents the Cyclic Steady State (CSS) of the system modeled. The concentration profiles of the SMBR are presented after 12 switches or 3 complete cycles. It is very clear that the extract stream and the raffinate stream are not exiting the system with the high purities desired. A small concentration of species C in the extract concentration history is visible. Also a small amount of undesired product D is present in the raffinate. As expected the system is not working in the optimum conditions. Performance parameters were not studied for this unit.

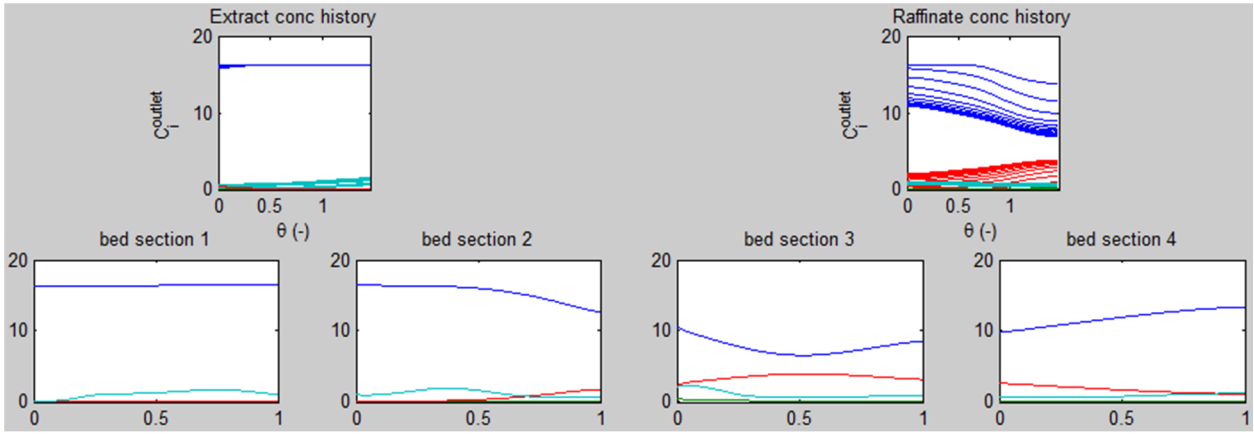

Figure 4-16 – SMBR in operation. Concentration histories of the outlets (top), concentration profiles along the 4 columns (bottom). The outlet profiles were written on top of previous profiles so that the cyclic steady state could be easily observed.

4.4. Comparison of FBCR and RFCR

The increased number of fractions collected with C (raffinate) in the RFCR, per run, is what differentiates it from FBCR. Another important detail is that the RFCR has twice the amount of packing of the FBCR since it is modeled has having two FBCR columns. Still other important aspect is that due to the accumulation of D near the feed, or in the central part of the RFCR, the regeneration step takes longer.

On Figure 4-17 it is suggested that for slower reactions, the productivity rapidly decreases and desorbent consumption gets too high lowering overall performance of the FBCR. This is mainly due to the smaller and smaller fraction that is collected as the reaction gets slower. For faster reactions the FBCR seems to compete with RFCR having similar desorbent consumption and about 20% higher productivity for $k' = 0.02 M^{-1} s^{-s}$.

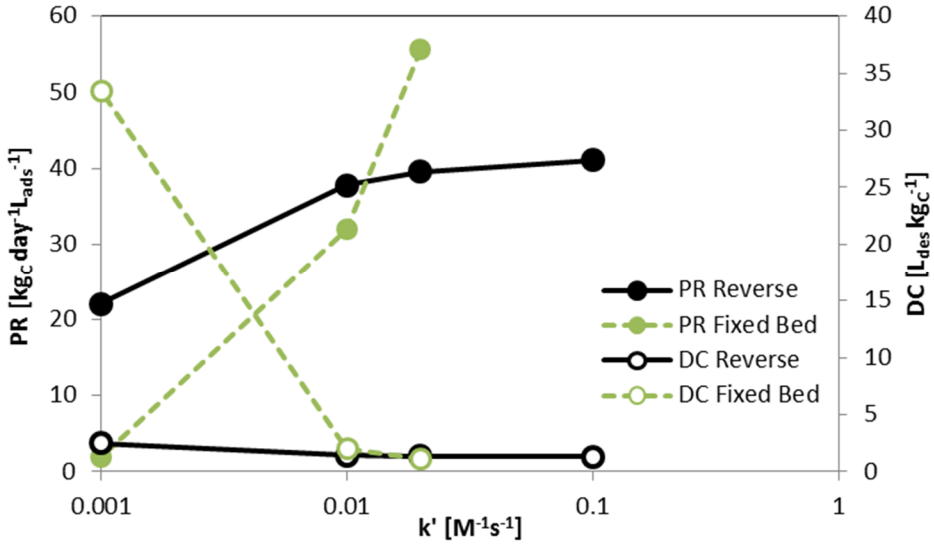

Figure 4-17 – Influence of kinetic constant in FBCR and RFCR productivity and desorbent consumption.

In Figure 4-18, while the FBCR is able to keep high purities and conversion on the spectrum of kinetic constants studied, the RFCR performance decreases as the reaction gets slower. The reactant B is not consumed before it reaches the end of the semi-bed. B is being lost, that is why the conversion decreases so sharply. Once again the extract purity remains high because at the end of the cycle, when it gets collected, all of the other species have already eluted.

In Figure 4-19, it is suggested that the RFCR would perform always better than the FBCR if the separation factor becomes lower (with productivity of RFCR being higher, and desorbent consumption being lower than the same parameters for the FBCR).

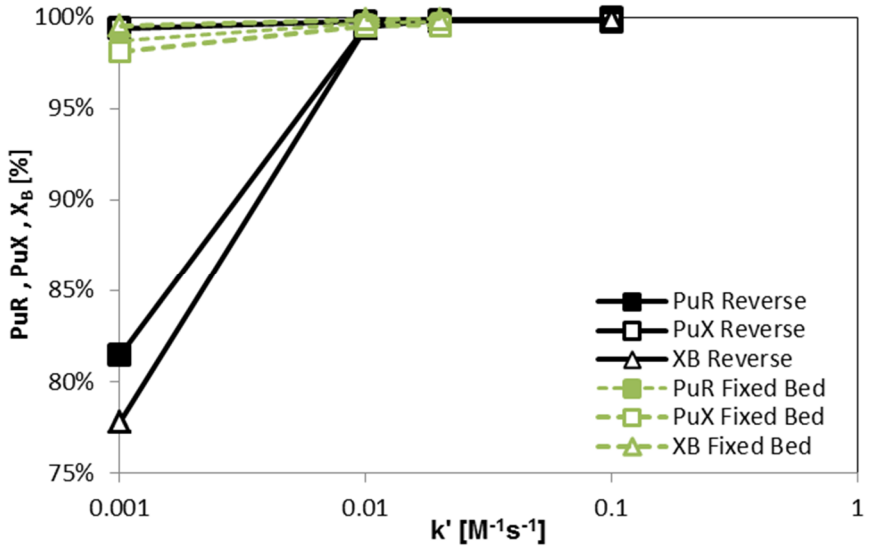

Figure 4-18 – Comparison of the influence of kinetic constant in FBCR and RFCR raffinate and extract purities and conversion of species B.

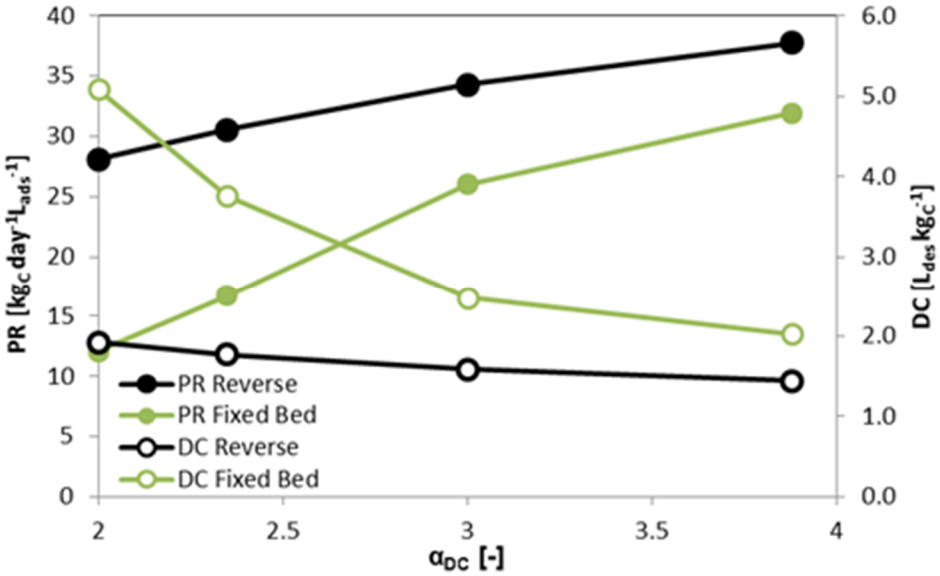

Figure 4-19 – Comparison of the influence of separation factor in FBCR and RFCR productivity and desorbent consumption.

In Figure 4-20, although all three performance parameters remain high, it is visible that for the FBCR, these do not start to decrease as the separation factor drops, as is the case for the RFCR. A justification for this to happen is that the RFCR has a fixed switch time to reverse the flow. During this set switch time, as the separation gets harder, it becomes easier for undesired species to elute.

For the FBCR that does not happen because the time at which the raffinate and extract get collected is set in each run, being optimized not to let the undesired species appear in the fractions collected.

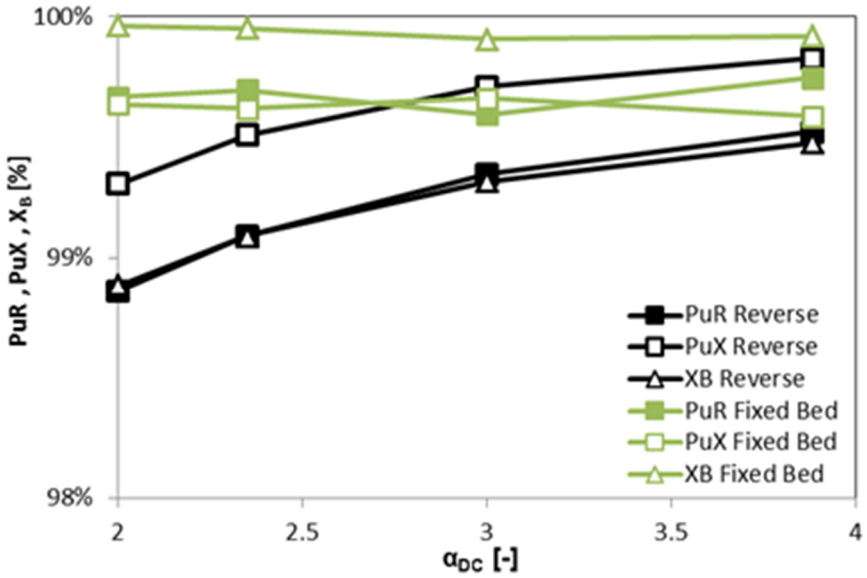

Figure 4-20 – Influence of separation factor in FBCR and RFCR raffinate and extract purities and conversion of species B.

5. Conclusions and Future Work

Simulation of Chromatographic Reactors was performed. The concepts of Fixed Bed, Reverse Flow and Simulated Moving Bed chromatographic reactors was explored for the equilibrium limited reaction of type $A + B \leftrightarrow C + D$, representing esterifications in a generic way. The model used to simulate all concepts was an equilibrium dispersive model.

Parametric sensitivity was made for the reaction kinetic constant, separation factor and switch time and results were evaluated as productivity of C, consumption of desorbent, conversion of B and purities of raffinate and extract. MATLAB® was used to perform the simulations which benefitted from its versatility and fast implementation.

The main conclusions taken from this work were:

- The MATLAB® *pdepe* is fast enough for preliminary calculations and dynamic modeling of chromatographic systems.
- The results of the simulations for the Reverse Flow Chromatographic Reactor (RFCR) were promising in the sense that it allows for a larger productivity with less desorbent consumption than the Fixed Bed Chromatographic Reactor (FBCR). The RFCR concept should be considered as an enhancement to reactions taking place in FBCR at lower reaction rates and at lower separation factors.
- If reactions are too slow, the advantages of the chromatographic reactor are not relevant, unless residence time is increased. Slower reactions do not favor the production and consequent removal of products from the reaction zone, so that equilibrium could be dislocated significantly. Chromatographic reactors should be used with high rates of reaction.
- Reactive mixtures with low separation factors treated in chromatographic reactors can still lead to high purity and high conversion parameters but at cost of a much lower productivity. The fractions can be shorter but still pure. For that RFCR should be compared to SMBR.

Since a comparison between simulation results and experimental work was not performed, it would be important to do that in the future, so that the validity of the results given by the simulations could be assessed. Additionally, consecutive reactions should also be studied.

The system for the simulation of SMBR was developed but was not optimized properly. In the future, efforts should be made in order to optimize this system.

Finally, it was found that the Finite Difference Method of computation provided by MATLAB® *pdepe* is fast enough for preliminary calculations, but its reliability should be tested with more accurate solvers that implement OCFEM for example.

References

Agar, Ruppel, 1988. Extended reactor concepts for dynamic DeNOx design. Chemical Engineering Science 43, 2073-2078.

Azevedo, D.C., Rodrigues, A.E., 2001. Design methodology and operation of a simulated moving bed reactor for the inversion of sucrose and glucose-fructose separation. Chemical Engineering Journal 82, 13.

Barker, P.E., Ganetsos, G., Ajongwen, J., Akintoye, A., 1992. Bioreaction-separation on continuous chromatographic systems. The Chemical Engineering Journal 50, B23-B28.

Borges da Silva, E.A., Ulson de Souza, A.A., de Souza, S.G.U., Rodrigues, A.E., 2006. Analysis of the high-fructose syrup production using reactive SMB technology. Chemical Engineering Journal 118, 167-181.

Falk, Seidel-Morgenstern, A., 2002. Analysis of a discontinuously operated chromatographic reactor. Chemical Engineering Science.

Falk, T., Seidel-Morgenstern, A., 1999. Comparison between a fixed-bed reactor and a chromatographic reactor. Chemical Engineering Science 54, 1479-1485.

Ganetsos, G., Barker, P.E., Alongwen, J.N., 1993. Batch and continuous chromatographic systems as combined bioreactor-separators, in: Ganetsos, G., Barker, P.E. (Eds.), Preparative and Production Scale Chromatography. Marcell Dekker, New York, pp. 375-394.

Javeed, S., Qamar, S., Seidel-Morgenstern, A., Warnecke, G., 2011. A discontinuous Galerkin method to solve chromatographic models. Journal of chromatography. A 1218, 7137-7146.

Javeed, S., Qamar, S., Seidel-Morgenstern, A., Warnecke, G., 2012. Simulation of Non-isothermal Reactive Chromatographic Processes, MATHMOD 2012 - 7th Vienna International Conference on Mathematical Modelling, Vienna, Austria.

Kawase, M., 2001. Lactosucrose production using a simulated moving bed reactor.

Kawase, M., Inoue, Y., Araki, T., Hashimoto, K., 1999. The simulated moving-bed reactor for production of bisphenol A. Catalysis Today 48, 199-209.

Kawase, M., Suzuki, T.B., Inoue, K., Yoshimoto, K., Hashimoto, K., 1996. Increased esterification conversion by application of the simulated moving-bed reactor. Chemical Engineering Science 51, 2971-2976.

Kurup, A.S., Subramani, H.J., Hidajat, K., Ray, A.K., 2005. Optimal design and operation of SMB bioreactor for sucrose inversion. Chemical Engineering Journal 108, 19-33.

Levan, Carta, 2008. Adsorption and Ion Exchange, Perry's Chemical Engineers' Handbook, 8 ed, p. 73.

Litto, R., Hayes, R.E., Sapoundjiev, H., Fuxman, A., Forbes, F., Liu, B., Bertrand, F., 2006. Optimization of a flow reversal reactor for the catalytic combustion of lean methane mixtures. Catalysis Today 117, 536-542.

Mai, P.T., Vu, T.D., Mai, K.X., Seidel-Morgenstern, A., 2004. Analysis of Heterogeneously Catalyzed Ester Hydrolysis Performed in a Chromatographic Reactor and in a Reaction Calorimeter. Industrial & Engineering Chemistry Research 43, 4691-4702.

Mazzotti, M., Neri, B., Gelosa, D., Morbidelli, M., 1997. Dynamics of a Chromatographic Reactor: Esterification Catalyzed by Acidic Resins. Industrial & Engineering Chemistry Research 36, 3163-3172.

Minceva, M., Gomes, P.S., Meshko, V., Rodrigues, A.E., 2008. Simulated moving bed reactor for isomerization and separation of p-xylene. Chemical Engineering Journal 140, 305-323.

Pereira, C.S.M., Zabka, M., Silva, V.M.T.M., Rodrigues, A.E., 2009. A novel process for the ethyl lactate synthesis in a simulated moving bed reactor (SMBR). Chemical Engineering Science 64, 3301-3310.

Podgornik, Tennikova, 2002. Chromatographic Reactors Based on Biological Activity, in: Scheper (Ed.), Modern Advances in Chromatography. Advances in Biochemical Engineering/Biotechnology, pp. 165-210.

Ray, A.K., Carr, R.W., 1995. Experimental study of a laboratory-scale simulated moving countercurrent moving bed chromatographic reactor. ChemScienceical Engineering Journal 50, 2195-2202.

Sainio, T., Zhang, L., Seidel–Morgenstern, A., 2011. Adiabatic operation of chromatographic fixed-bed reactors. Chemical Engineering Journal 168, 861-871.

Sardin, M., Villermaux, J., 1985. Synthèse de l'acétate de menthyle par chromatographie réactive. The Chemical Engineering Journal 30, 91-101.

Silva, V.M.T.M., Rodrigues, A.E., 2005. Novel process for diethylacetal synthesis. AIChE Journal 51, 2752-2768.

Silveston, P.L., Hudgins, R.R., 2012. Periodic operation of reactors. Butterworth-Heinemann,, Oxford, p. 1 online resource (608 p.).

Sircar, S., Rao, M.B., 1999. Liquid-phase sorption-enhanced reaction process. AIChE Journal 45, 2326-2332.

Tonkovich, A.L.Y., Carr, R.W., 1994. A simulated countercurrent moving-bed chromatographic reactor for the oxidative coupling of methane: Experimental results. Chemical Engineering Science 49, 4647-4656.

Viecco, G.A., Caram, H.S., 2006. Comparison between simulated moving bed and reverse flow chromatographic reactors for equilibrium limited reactions. Chemical Engineering Science 61, 6869-6879.

Vu, T.D., Seidel-Morgenstern, A., 2011. Quantifying temperature and flow rate effects on the performance of a fixed-bed chromatographic reactor. Journal of chromatography. A 1218, 8097-8109.

Yu, W., Hidajat, K., Ray, A.K., 2003. Optimal operation of reactive simulated moving bed and Varicol systems. Journal of Chemical Technology & Biotechnology 78, 287-293.

Zhang, Z., Hidajat, K., Ray, A.K., 2001. Application of Simulated Countercurrent Moving-Bed Chromatographic Reactor for MTBE Synthesis. Industrial & Engineering Chemistry Research 40, 5305-5316.

A. Appendix

Table A-1 – Performance parameters for the FBCR run #2.

run #2 simulations	1	2	3	4	5
PR [$kg_C\ day^{-1}\ L_{ads}^{-1}$]	25.67	21.90	32.19	24.87	25.18
DC [$L_{des}\ kg_C^{-1}$]	2.39	2.82	1.89	2.64	2.59
PuR	99.82%	99.61%	99.32%	99.72%	99.73%
PuX	99.60%	99.57%	99.87%	99.61%	99.60%
X_B	99.96%	99.90%	99.85%	99.94%	99.94%

Table A-2 - Performance parameters for the FBCR run #3.

run #3 simulations	1	2	3	4	5
PR [$kg_C\ day^{-1}\ L_{ads}^{-1}$]	18.69	15.72	16.74	17.19	17.14
DC [$L_{des}\ kg_C^{-1}$]	3.42	3.86	3.62	3.78	3.78
PuR	99.78%	99.66%	99.70%	99.71%	99.72%
PuX	99.42%	99.61%	99.63%	99.59%	99.64%
X_B	99.96%	99.95%	99.96%	99.95%	99.96%

Table A-3 - Performance parameters for the FBCR run #4.

run #4 simulations	1	2	3	4
PR [$kg_C\ day^{-1}\ L_{ads}^{-1}$]	13.76	11.36	12.06	12.76
DC [$L_{des}\ kg_C^{-1}$]	4.75	5.27	4.97	5.02
PuR	99.75%	99.67%	99.66%	99.66%
PuX	99.26%	99.64%	99.63%	99.63%
X_B	99.96%	99.96%	99.96%	99.96%

Table A-4 - Performance parameters for the FBCR run #5.

run #5 simulations	1	2	3	4
PR [$kg_C\ day^{-1}\ L_{ads}^{-1}$]	63.43	50.80	57.18	58.72
DC [$L_{des}\ kg_C^{-1}$]	0.99	1.24	1.10	1.15
PuR	99.88%	99.79%	99.85%	99.82%
PuX	99.59%	99.59%	99.59%	99.62%
X_B	99.96%	99.90%	99.99%	99.98%

Table A-5 - Performance parameters for the FBCR run #6.

run #6	1
PR [$kg_C\ day^{-1}\ L_{ads}^{-1}$]	1.87
DC [$L_{des}\ kg_C^{-1}$]	33.54
PuR	98.78%
PuX	98.16%
X_B	99.57%

Table A-6 – Properties for the species of the system considered.

species	MW_i [g mol]	ρ_i [g cm^{-3}]	C_{pure} [M]
A (ethanol)	46.07	0.789	17.1
B (lactic acid)	90.08	1.206	13.4
C (ethyl lactate)	118.13	1.034	8.8
D (water)	18.02	0.998	55.4

Conversion on equilibrium (catalyst only)

Given an equilibrium constant of K_{eq} = 1.4 at 323.15 K, which is the same for the system considered in this work, $A + B \leftrightarrow C + D$, and a reactant mixture of concentrations $C_A = C_B = 7.51\ M$, given a certain length, the equilibrium conversion is reached.

Table A-7 – Conversion of reagent B calculation table with K_{eq}=1.4, for the system considered**.**

A	B	C	D
7.514	7.514	-	-
$7.514 - x$	$7.514 - x$	x	x

The conversion for the equilibrium is given by

$$K_{eq} = \frac{C_C^{eq} C_D^{eq}}{C_A^{eq} C_B^{eq}} \leftrightarrow 1.4 = \frac{x^2}{(7.514 - x)^2} \leftrightarrow x \approx 4.072$$

So the maximum attainable conversion is

$$X_B(\%) = \frac{4.072}{7.514} \times 100 \approx 54\%$$

Matching stoichiometry in the mixture Recycle to feed again - FBCR

Thee fractions defined as mixture recycle need to be set to the stoichiometric ratios in order to be fed again. An example is given for the first and second feed cycles.

$\tau = 50\ s$	$Q_{feed} = 1.062\ cm^3/s$

The initial feed has composition of $C_A = C_B = 7.51\ M$ and since the duration of the feed is going to be $\theta = 1.6$ the volume to be fed, given the flow is constant is

$$V_1 = 1.6 \times \tau \times Q_{feed} \approx 85\ cm^3$$

The amount of material to be recycled from this runs is composed of n_A = 0.300 mol, n_B = 0.070 mol, n_C = 0.369 mol and n_D = 0.009 mol. So we need to add $n_{A,add}$ and $n_{B,add}$ to make up the same volume to be fed again. The volume resulting from the new composition is given by

$$V_2 = \sum_i^n \frac{n_i \times MW_i}{\rho_i}$$

So, then a function to minimize with the MS Excel solver is set,

$$solver\ function = (x_A - x_B)^2 + (1 - x_A + x_B + x_C + x_D)^2 + (V_1 - V_2)^2$$

Table A-8 –Composition of fraction recycle after makeup material is added; Values are for the simulated run #1.

Component	Feed composition	Composition after makeup 1	Composition after makeup 2	Composition after makeup 3	Composition after makeup 4
C_A	7.514	3.775	5.782	4.695	5.286
C_B	7.514	3.775	5.782	4.695	5.286
C_C	0	4.339	2.013	3.275	2.590
C_D	0	0.100	0.026	0.056	0.038